2020-03-16

LOSS REDUCTION AND VOLTAGE STABILITY ENHANCEMENT OF DISTRIBUTION NETWORK THROUGH OPTIMAL ALLOCATION OF DISTRIBUTION STATCOM CASE STUDY (BAHIR DAR DISTRBUTION NETWORK)

YISAYE, NEBIYU

BAHIR DAR UNIVERSITY

BAHIR DAR INSTITUTE OF TECHNOLOGY

SCHOOL OF RESEARCH AND POSTGRADUATE STUDIES

FACULTY OF ELECTRICAL AND COMPUTER ENGINEERING

POST GRADUATE PROGRAM IN POWER SYSTEM ENGINEERING

LOSS REDUCTION AND VOLTAGE STABILITY ENHANCEMENT OF DISTRIBUTION NETWORK THROUGH OPTIMAL ALLOCATION OF DISTRIBUTION STATCOM

CASE STUDY (BAHIR DAR DISTRBUTION NETWORK)

NEBIYU YISAYE KINDYE

Bahir Dar, Ethiopia

June, 2019

LOSS REDUCTION AND VOLTAGE STABILITY ENHANCEMENT OF DISTRIBUTION NETWORK THROUGH OPTIMAL ALLOCATION OF DISTRIBUTION STATCOM

CASE STUDY (BAHIR DAR DISTRBUTION NETWORK)

BY

NEBIYU YISAYE KINDYE

A thesis submitted to the school of Research and Graduate Studies of Bahir Dar Institute of Technology, BDU in partial fulfillment of the requirements for the degree of master in the Power System Engineering in the Faculty of Electrical and Computer Engineering.

Advisor

Dr-Ing Belachew Bantyirga

Bahir Dar, Ethiopia

June, 2019

DECLARATION

I, the undersigned, declare that this thesis comprises my own work. In compliance with internationally accepted practices, I have acknowledged and refereed all materials used in this work. I understand that non-adherence to the principles of academic honesty and integrity, misrepresentation/ fabrication of any idea/data/fact/source will constitute sufficient ground for disciplinary action by the university and can also evoke penal action from the sources which have not been properly cited or acknowledged.

Name of the student: Nebiyu Yisaye Kindye

Signature _____

Date of submission: 02/07/2019

Place: Bahir Dar

This thesis has been submitted for examination with my approval as a university advisor.

Advisor Name: Dr-Ing Belachew Bantyirga

Advisor's Signature_____

NEBIYU YISAYE KINDYE

LOSS REDUCTION AND VOLTAGE STABILITY ENHANCEMENT OF DISTRIBUTION NETWORK THROUGH OPTIMAL ALLOCATION OF DISTRIBUTION STATCOM

CASE STUDY (BAHIR DAR DISTRBUTION NETWORK)

Bahir Dar University

Bahir Dar Institute of Technology

School of Research and Graduate Studies

Faculty of Electrical and Computer Engineering

THESIS APPROVAL SHEET

Student: Nebiyu Yisaye _____ 02.07.2019

Name Signature Date

The following graduate faculty members certify that this student has successfully presented the necessary written final thesis and oral presentation for partial fulfillment of the thesis requirements for the Degree of Master of Science in Power Systems Engineering.

Approved By:

Advisor: Dr.-Ing. Belachew Bantyirga _____ 03/07/2019.

Name Signature Date

External Examiner: Dr.-Ing. Getachew Biru _____ 02.07.2019

Name Signature Date

Internal Examiner: Dr.Tassew Tadiwos _____ 03/07/2019

Name Signature Date

Prog. Chair Holder: Mr.Tewdros Gera _____ 03/07/2019

Name Signature Date

Faculty Dean: Mr. Solomon Luta _____ 03/07/2019

Name Signature Date

ACKNOWLEDGMENT

First of all, I would like to thank the Almighty God Allah for his provision of grace to complete the entire work. Next, I would like to express my deepest gratitude and appreciation to my advisor Dr-Ing Belachew Bantyirga, for his guidance and encouragement. His patience and support have enabled me to achieve my highest potential in both academic and professional work. My sincere thanks to Bahir Dar substation II EEU employees for their support in obtaining the tools and data necessary for conducting my research and for facilitating my schedule.

ABSTRACT

This work presents the way of improving the performance of the distribution network by maintaining voltage profile, voltage stability, and reduction of power loss via injecting reactive power through the network. D-STATCOM is commonly used in the distribution system for reactive power compensation so that it improves voltage profile, reduces power losses, and also improves the system voltage stability. The study of this work was conducted on papyrus feeder which has 59-bus, 47 loads, and a total capacity of 3.9 MW. The voltage profiles of most buses are not in an acceptable range, and the voltage stability index of the buses shows that network is prone to voltage stability problem. The active and reactive power loss of the feeder is 131.72 KW and 111.35 KVAr respectively. The optimal D-STATCOM allocation in electric distribution system enhances in maximizing energy utilization, feeder loss reduction, voltage stability, and profile improvement. To allocate power control variables in the best possible location and with proper size two solution methods are applied. As the first method, the weakest bus of the system was selected for the optimal placement of D-STATCOM using bus based voltage stability index analysis. In the second method, Particle swarm optimization (PSO) was applied for selecting optimal placement and size of D-STATCOM. The PSO optimization algorithm formulates a problem by considering system loss reduction, enhancement of voltage profile and voltage stability index of the operated network. A direct load flow analysis also carried out for the purpose of total system loss and bus voltage magnitude determination before and after compensation with D-STATCOM. The optimal allocation problem was tested in different system cases based on the number and size of D-STATCOM. By comparing the net cost of D-STATCOM in relation to total system loss reduction single D-STATCOM installation has a better system performance. After the installation of single D-STATCOM with an optimal allocation through the feeder, the voltage profile of the system improved between 0.95-1.05 p.u. The voltage stability index of the operated network increases as compared with base case stability. The active and reactive power loss through the line reduced to 25.03% and 25.25% respectively. The compensating device cost analysis indicates that the total cost coverage will take 6.7 years and it is an optimum solution.

Keywords: Distribution static synchronous compensator**,** Forward-Backward load flow, Loss Reduction, Particle swarm optimization, Voltage stability, Voltage profile

Table of Contents

LIST OF ABBREVIATIONS

AAC	All Aluminum Conductors
ABC	Artificial Bee Colony
AC	Alternate current
ACO	Ant Colony Algorithm
AVR	Automatic voltage regulator
BCBV	Branch Current to Bus Voltage
BFOA	Bacterial Foraging Optimization algorithm
BIBC	Bus Injected to Branch Current
CI	Constant Current
CP	Constant Power
CZ	Constant Impedance
DC	Direct current
DFC	Dynamic Flow Controller
DG	Distribution Generator
D-STATCOM	Distribution Static synchronous compensator
DT	Distribution Transformer
EEU	Ethiopian Electric Utility
ESA	Exhaustive Search algorithm
FACTS	Flexible AC Transmission System
GA	Genetic Algorithm
GMR	Geometrical Mean Radius
GTO	Get turns off
HAS	Harmony search algorithm
HVDC	High-voltage direct current
IA	Immune algorithm
IEEE	Institute of Electrical and Electronics Engineers
IGBT	Insulated-gate bipolar transistor
KCL	Kirchhoff's Current Law
KVL	Kirchhoff's Voltage Law
LT	Lower Transmission
MOSFETS	Metal-Oxide-Semiconductor Field Effect Transistor

MSFLA	Modified Shuffled Frog Leaping Algorithm
PCC	Point of Common Coupling
PLI	Power Loss index
PSO	Particle Swarm Optimization
PU	Per unit
PV	Photovoltaic
PWM	Pulse with modulation
RDS	Radial Distribution System
SCRS	Silicon controlled rectifiers
SSSC	Static Synchronous Series compensator
SVC	Static Var Compensator
TCSC	Thyristor Controlled Series Compensator
UPFC	Unified Power Flow Controller
UPQC	Unified power quality control
VSC	Voltage Source Converter
VSI	Voltage source inverter

LIST OF SYMBOLS

GMR_a	Geometric mean ratio of conductor a
r	Actual conductor radius r
D	Distance between conductors
D_{ab}	Distance between conductors a and b
D_{bc}	Distance between conductors b and c
D_{ac}	Distance between conductors a and c
k	GMR factor
Z_a	Impedance of conductor a
R_a	Resistance of conductor a
θ	Angle between current and voltage
C_1	Weight coefficient
C_2	Weight coefficient
$G_{best\ id}$	Group best position
$P_{best\ id}$	Particles best position
S_{id}^{k}	Current searching point
S_{id}^{k+1}	Modified searching point
V_{id}^{K+1}	Current velocity
$\mathbf{W_{max}}$	Maximum weight
$\mathbf{W_{min}}$	Minimum weight
F_1	Objective function for loss reduction
F_2	Objective function for voltage profile
F_3	Objective function for voltage stability
HZ	Hertz
I_{DS}	Current injected by D-STATCOM
I_i	Portion current on line
I_{ij}	Current flows from bus i to bus j

K	Current iteration
Km	Kilometer
K_{max}	Maximum current iteration
KV	Kilovolt
KVA	Kilovolt Ampere
KVAr	Kilovolt Ampere reactive
KW	Kilowatt
KWh	Kilowatt-hour
L_i	Portion length of the line (km)
ms	Millisecond
MVA	Mega Volt Ampere
MVAr	Megavolt Ampere reactive
MW	Megawatt
n	Number of particles in a group
Ploss	Active power loss
Qloss	Reactive power loss
R	Resistance
r	Random number
R_i	Resistance of the line (Ohm/km)
V	Volt
V_i	Line voltage of bus i
Vs	System Voltage
Vsc	Voltage of source converter
W_1	Weighting coefficient for power loss reduction
W_2	Weighting coefficient for voltage profile
W_3	Weighting coefficient for voltage stability
X_i	Reactance of the line (Ohm/km)

LIST OF FIGURES

LIST OF TABLES

CHAPTER ONE

1. INTRODUCTION

1.1 Background

Power system networks are becoming very complex, dynamic, nonlinear, and are prone to various types of disturbances. The distribution system is part of a power system that distributes power to end users. It is the most extensive part of the electrical system as a result of being responsible for energy losses.The distribution network is constantly being faced with an ever-growing load demand; thus increasing load demand is resulting in increased burden and reduced voltage profile. It has also a typical feature that the voltages at buses reduce if we move away from substation. In a certain industrial area under critical loading, it may lead to voltage collapse. Whenever there is a change in load the system voltage level changes with the drop in voltage level,the reactive power demand increases.If the reactive power demand is not met,then its leads to further decline in bus voltage result in cascading effect on neighboring regions,thus to improve the voltage profile and to avoid voltage collapse reactive power compensation is required.

The distribution network of Bahir Dar city is characterized by radial, long distance, and poor reactive power compensation, some of which may risk total or partial collapse in the event of major disturbances and experience low voltage under heavy load. There is also a high customer's turnout incorporating hundreds of customers connected to the existing system. Thus more customers are going to be connected to the existing network; this may lead to overloading, high-power loss in some of the lines and system equipment's and consequently reduces system efficiency, degrading voltage profile and reliability.

A Dramatic increase in demand for energy has caused suppliers of energy to search for a quicker and relatively less expensive means of improving the declining reliability and stability of distribution power networks. There are a lot of indications that shows the electric power distribution is very low in Bahir Dar city. The industries, commercials, and residential end users are facing frequently power interruption, voltage variation/under voltage, working with poor power factor, voltage unbalances, etc. The drop of the voltage is causing, heating of the motors, early failure of equipment, overvoltage causes damage of electronic devices. This has brought about the motivation to choose the option of Distributed D-STATCOMs as a compensation tool for loss reduction and stability improvement.

The increase in the loading of the distribution lines and components can also lead to voltage collapse and poor voltage profile due to the shortage of reactive power delivered at the load centers. A system enters a state of voltage instability when a disturbance occurs, an increase in load demand or change in system condition causes a progressive and uncontrollable decline in voltage. The main factor causing instability is the inability of the power system to meet the demand for reactive power. Maintaining an adequate voltage level economically is the primary facing problem. They are holding the determined probable capacity for their bulk distribution system to avoid the charge of building new lines and generation amenities[1].

At a time when a bulk distribution system is functioned close to the voltage instability limit, it turns out to be difficult to control the reactive power margin for that system. As a consequence, the system stability becomes major concerns and an appropriate way must be found to monitor the system and voltage collapse. Voltage instability problems can be solved by providing adequate reactive power support at an appropriate location in the system. To match the reactive power demand and thus to improve voltage profile and voltage stability of the operated network optimal placement of the Flexible AC Transmission System (FACTS) controllers provides an alternate solution[2].

The concept of FACTS was first defined by Hingorani in 1988.They are basically power electronics based devices that are incorporated in the power system with an objective of enhancing transmission capacity and controlling several parameters of the transmission network[3][2]. In order to increase system performance in loss reduction, improvement of voltage profile and stability there should be an installation of highly advanced equipment; Such equipment's are capacitor banks, shunt and series reactors, Automatic Voltage Regulator (AVR) or recently developed Distribution Network Flexible AC Transmission (FACTS) such as Distribution Static Compensator (D-STATCOM), Unified Power Quality Controller (UPQC), and Static Synchronous Series Compensator (SSSC). Compare with other reactive power compensation devices; D-STATCOM has better features, such as low power losses, less harmonic production, high regulatory capability, low cost, and compact size[4].

1.2 Statement of the Problem

Distribution networks are well known for their high R/X ratio and significant voltage drop that could cause substantial power losses along with the feeders. Studies have indicated that as much as 13% of total power generated is wasted in the form of losses at the distribution level[5]. The electrical energy demand growth in Bahir Dar distribution network has been enormous in the past few years as a result of the expansion of industry, an increment of power consumption, building of new feeders, and expansion of existing feeder lines. The continuous demand in electrical power system network causes the system to increases loading of the equipment, operating in unbalanced voltage condition, increased voltage drops, and damages of protective devices. The active and reactive power loss of the feeder is 131.72 KW and 111.35 KVAr respectively. The level of voltage and stability of power supplied at the extreme end of the feeder is significantly low. This research has confirmed that 47% of bus voltage has low level of voltage deviation. Moreover, this weak voltage profile leads the system to high power loss. As a result, a voltage that is not at its limit causes voltage instability and blackout. At certain loading, the voltage drop is not maintained, and it caused a weak voltage profile. So, to improve the voltage profile, and to minimize the power loss, a scientific solution is highly required. Therefore, a method must be devised for a quicker and relatively less expensive means of improving the declining reliability and stability of power distribution networks. Enhancement of distribution power system performance can be maximized by installing D-STATCOM in the RDS. Thus installing a compensating device plays an important role in delivering power to different customers and industries in more secure and reliable ways for Bahir Dar city feeders.

1.3 Objectives of the study

1.3.1 General Objective

The General objective of this research deals with loss reduction, voltage profile, and voltage stability enhancement of Bahir Dar distribution network through optimal allocation of D-STATCOM using Particle swarm optimization.

1.3.2 Specific Objective

The specific objectives are:

- To analyze system load flow analysis using direct load flow method.
- To model D-STATCOM in radial distribution network feeder.
- To simulate the optimization problem using Mat lab software.
- To analyze optimal placement and sizing of D-STATCOM using the PSO method.
- To compare the results of system performance with and without D-STATCOM.

1.4 Methodology

The following steps which comprise the methodology adopted for this research work are:

Literature review: It includes reading journals, books and other documents in related areas.

Acquire the relevant network data: line data, bus data, network base voltage, conductor sizes and impedance definitions, lengths, loadings.

System Modeling: Bahir Dar distribution power system feeder with D-STATCOM was modeled for system analysis.

Data analysis: Using Mat lab simulation software the load flow and optimization algorithm finds an optimal system performance and allocation of D-STATCOM respectively.

Result Analysis

- Analyzing system performance by considering different system cases.
- Result Comparison of the objective functions (loss reduction, voltage profile, and stability) before and after compensation with single and multiple D-STATCOMs.

Conclusion and discussion

- Finally, the result of this thesis will be discussed and concluded.
- Recommendation for future works.

1.5 Scope of the study

The installation of D-STATCOM in the distribution system improves both the transient and steady-state performances. This study focuses on the real power loss minimization, voltage profile, and voltage stability improvement of distribution feeders by optimal placing and sizing of D-STATCOM using particle swarm optimization. The scopes of this work are simulating the proposed system through Mat lab simulation software and analyze the system performance enhancement before and after compensating using D-STATCOM.

1.6 Significance of the thesis

The proposed study offers a power system performance enhancement solution to end users providing sustainable electricity in a good manner. Moreover, the technology adopted also provides potential technology transfer opportunities to various academic and technical institutions through which training and livelihood of stakeholders may be enhanced.

- It improves system capacity and hence permits additional loads (motors, lighting, etc.) to be added without overloading the system.
- To show D-STATCOM is the best-compensating device for improving distribution system performance like loss reduction, voltage profile, voltage stability, and power factor improvement.

1.7 Outline of the thesis

The thesis is organized into six chapters which are briefly summarized below.

In **Chapter 1**, introduction and the problems observed on distribution feeders have stated clearly. In addition to this, the overall objectives, scopes and the methods used for achieving the main objective have shortly summarized.

Chapter 2, gives a short summary of extensive literature reviews.

Chapter 3, general theoretical backgrounds have discussed. It discusses the distribution power system, power flow, distribution Statcom, system modeling, and optimization algorithms.

In **Chapter 4**, the general methodology of this work was stated.

In **Chapter 5,** result and discussion were discussed.

Finally, **Chapter 6** concludes the work is done and the results obtained. Recommendations for future work were also presented.

CHAPTER TWO

2. LITERATURE REVIEW

A review of several authors works is done on the optimal placement and sizing of D-STATCOM for improving the performance of the distribution network [6][7].
Farhoodnea et al. (2013) presented a novel approach for optimal D-STATCOM placement in radial distribution networks using the Firefly Algorithm. In this work, total harmonic distortion, average voltage deviation, and total investment cost are considered as the objective functions. The performance of the proposed technique was tested in the IEEE 16-bus system. It was reported that it produces a superior result when compared with PSO and GA algorithms[8].

Hussain and Subbaramiah (2013) proposed an effective analytical method for the optimal location of D-STATCOM in the radial distribution system for power loss minimization and voltage profile improvement. In this work, a backward-forward sweep technique was applied for load flow analysis. The D-STATCOM was modeled and its size determined by assuming a voltage magnitude of 1p.u. at the candidate node. An objective function comprising of total system losses and system voltage profile was used for the optimal location of D-STATCOM. This method was tested on a standard IEEE 33-bus radial distribution system[9].

Jain et al. (2014) presented an improved analytical method approach for power loss reduction. It considered load current, BIBC matrix and forward sweep for power flow analysis. The power flow was performed by implementing the compensating values for constant power (CP), constant current (CI), constant impedance (CZ) and finally a composite load of 30% constant impedance, 20% Constant current, 50% constant power load. A sensitivity-based approach to the optimal placement of D-STATCOM was adopted. This method was tested on a standard IEEE 33-bus radial distribution system and has a better performance compared with the analytical method[10].

Taher and Afsari (2014) proposed a novel approach to the optimal location and sizing of D-STATCOM for power loss reduction in radial distribution systems by an immune algorithm (IA).In their work, the backward/forward sweep technique was used for load flow calculations.

An objective function comprising of the total cost of power loss, D-STATCOM installations, deviation of node's voltage, and line's current was formulated. The D-STATCOM was modeled with an assumed voltage magnitude of 1p.u. at the candidate node, while the IA was employed to determine the optimal size of D-STATCOM. The results of the proposed approach as tested on standard IEEE 33 and 69-bus radial distribution systems were found to perform better when compared to GA[11].

Kumarasamy and Raghavan (2014) proposed a cost-effective solution for optimal placement and size of multiple STATCOM using particle swarm optimization. The objective function incorporates system parameters like voltage profile, system loss, reactive power compensation, and system voltage stability. In contrast with conventional optimization problems, the magnitude of the weighting for the sub-objective function is chosen by the real-time cost or penalty value. The IEEE 30 bus system is taken as a test system and Newton Rapson load flow was carried out for power flow analysis. The placement of multiple STATCOM in the network was varied as the weight of the objective functions varies[12].

Balu et al. (2014) state an effective method to identify the optimum location and size of D-STATCOM using Fuzzy logic method for minimizing the loss and voltage profile improvement. The optimal size of D-STATCOM is calculated by modeling it to maintain the voltage magnitude as 1p.u and to supply required reactive power for compensation at the node where it's placed. Forward-backward load flow analyses were carried out for the analysis of bus voltage and loss calculation. The IEEE-33 bus test system is considered for this study. It examines a high reduction of power loss and voltage profile improvement in RDS [13].

Yuvaraj et al. (2015) investigated an optimal placement and sizing of D-STATCOM using harmony search algorithm. Power loss minimization is a single objective function that is considered as an optimization function. The proposed work was tested in the IEEE 33-bus system. It uses a direct approach of BIBC matrix for load flow analysis. The proposed work compares the annual total loss of RDS before and after installation with D-STATCOM. The real and reactive power loss has been reduced to a percentage reduction of 28.97% and 28.67% respectively[4].

Gupta and Kumar, (2015) presented an analytical approach for determining the optimal

location and size of D-STATCOM for radial distribution networks with the aim of reducing loss, improving voltage profile and overall energy saving. Two different sensitivity methods: the power loss index (PLI) and voltage stability index (VSI) were applied to determine the optimal location of D-STATCOM. The optimal size of D-STATCOM was calculated using the vibrational technique. This approach was carried out on a standard IEEE 33-bus test system[14].

Devabalaji and Ravi (2015) proposed a novel approach for optimal location and sizing of multiple DGs and D-STATCOM in radial distribution systems based on the combination of LSF and BFOA method. The research considered a predetermined location for DGs and D-STATCOM using LSF, while the optimal size is determined using BFOA. A multi-objective function comprising of power loss, voltage profile index and operational cost of the system is minimized. Analysis with eight different cases was carried out on two standard IEEE test networks (33 and 169 -bus) using the proposed method. Results obtained from the different analyses indicated a better superiority of the proposed approach over others used in past works[15].

Atma et al. (2015) presented a modified power loss index method for the optimal location and size of D-STATCOM for the reduction of power loss and improvement of the voltage profile. First, the load flow analysis is conducted on a radial distribution system for calculating line losses and voltage profile. After this, the size of D-STATCOM is determined by steady-state mathematical modeling. Then the power loss index is applied for finding the optimal location of the device. The bus with the highest value of PLI (power loss index) value is selected as the candidate bus. Finally, the Newton Rapson load flow is carried out by compensating the obtained size of D-STATCOM at the candidate bus for the three IEEE test system. The result showed that the reduction in power loss as well as improvement in the voltage profile of the system[16].

Joseph Sanam et al. (2016) proposed the optimal allocation of D-STATCOM and DG in a radial distribution network using the exhaustive search algorithm. The problem formulated for allocation of DG and D-STATCOM is integrated into the Forward-Backward sweep load flow algorithm to study the impact of allocation devices.

The effectiveness and performance of the proposed method were tested on IEEE 33-

bus distribution system. Some range of active and reactive power simultaneously injected at each node of distribution by corresponding the size and location of DG and D-STATCOM respectively[17].

Mohammed and Srinivasula (2016) proposed an optimal placement of STATCOM using an artificial bee colony (ABC) algorithm. In this work, an objective function of minimizing power losses, installation cost, voltage deviation, and fuel cost minimization of the network subject to equality and inequality constraint was formulated. The proposed system tested in the IEEE 30 bus system and the simulation result showed that the optimal placed D-STATCOM by the ABC algorithm was effective to maintain the voltage profile, minimizes the deviations and reduces power loss[18].

Domkawale and Chandrakar (2017) proposed a method for voltage stability enhancement for large power systems using STATCOM. This work takes a PV curve of a power system to identify the stable and unstable operation at the different buses of the IEEE 57-bus system. Along with the PV curve, the L-index (line stability index) method is used which determines the line stability factor shows best optimum location to place the Statcom. The Newton Rapson load flow analysis method was applied for the calculation of the bus voltage profile. The result clearly showed that by optimal located Statcom using the L-index method provides large changes in voltage profile and stability index[19].

The reviewed works of literature state different methods for an optimal allocation problem. Thus studies have certain limitations like single objective function, long algorithm simulation time, values of the weighting factors for multi-objective functions were simply taken based on theoretical assumptions, fails to consider the cost of DSTATCOM integration, not clearly present the necessary network constraints, and other associated benefits have not been considered while solving the location and sizing problems. This research fills the gap of previous works in the area of optimal placement and sizing of D-STATCOM like multi-objective optimization function, fast convergence characteristics of PSO algorithm, impact of integrating D-STATCOM on economical biases, and system constraints for PSO simulation.

CHAPTER THREE

3. THEORETICAL BACKGROUND

3.1 Distribution system

An electric supply system consists of three principal components. That is, the generation station, the transmission and the distribution system. The distribution power system is the electrical system between the substation fed by the transmission system and the consumer meters. It generally consists of feeders, distributors and the service mains. The Ethiopian Electric power utility system has 400KV, 230KV, 132KV primary transmission systems, 66kV, and 45kV as a sub-transmission system and 33kV and 15kV as a distribution system. At all the 66 or 45kV substation power transformers of various ratings like 25 /12 /6.3/3MVA are installed in step down voltage of 15kV for feeding the Distribution Transformers (DT). The outgoing feeders are connected in a radial fashion.

3.2 Power loss in the distribution system

It is a well-known fact that not all energy supplied to a distribution utility reaches the end consumer. A substantial amount of energy is lost in the distribution system by way of technical and non-technical losses. The distribution system accounts for the highest technical and non-technical losses in the power sector[20].

3.2.1 Technical Losses

Technical losses are caused by the physical properties of the components of the power system. The most obvious example is the power dissipated in transmission lines and transformers due to internal electrical resistance. Technical losses are naturally occurring losses (caused by action internal to the power system) and consist mainly of power dissipation in electrical system components such as transmission lines, power transformers, measurement systems, etc. Technical losses are possible to compute and control, provided the power system in question consists of known quantities of loads.
These include resistive losses of the primary feeders, the distribution transformer losses (resistive losses in windings and the core losses), resistive losses in secondary network, resistive losses in service drops and losses in kWh meter [21].

Losses are inherent to the distribution of electricity and cannot eliminate. Technical

losses are due to current flowing in the electrical network and generate the following types of losses:

- Copper losses: those are due to I^2R losses that are inherent in all inductors because of the finite resistance of conductors.
- Dielectric losses: are losses that result from the heating effect on the dielectric material between conductors.
- Induction and radiation losses: these losses have produced by the electromagnetic fields surrounding conductors.

The causes of technical losses are:

- Harmonics distortion
- Long single phase lines
- Unbalanced loading
- Losses due to overloading and low voltage
- Losses due to the poor standard of equipment

3.2.2 Non-Technical Losses

Non-Technical losses are caused by actions external to the power system or caused by loads and conditions that the technical losses computation failed to take into account. It is more difficult to measure because these losses are often unaccounted for the system operators and thus have no recorded information [22].

Measures for reducing technical losses:

- Identification of the weakest areas in the distribution system and improving using compensation equipment.
- Reducing the length of LT lines by the relocation of distribution substations/installations of additional distribution transformers (DTs).
- Installation of lower capacity distribution transformers at each consumer premises instead of cluster formation and substitution of DTs with those have lowered no-load losses such as amorphous core transformers.

3.3 Voltage profile improvement

In a power system, the system operator is obligated to maintain the voltage level of each customer bus within the required limit. To ensure voltage profiles are satisfactory in distribution systems, different standards have been established to provide stipulations or recommendations. Actually, in practice, many electricity companies try to control voltage variations within the range of ±5%. One of the upcoming widely adopted methods for improving voltage profiles of distribution systems is introducing distribution Statcom (D-STATCOM) in distribution systems. The D-STATCOM units improve voltage profiles by changing power flow patterns. The locations and sizes of D-STATCOM would have a significant impact on the effect of voltage profile enhancement[23].

3.4 Voltage stability improvement

Voltage stability has become one of the main concerns to maintain system security in power system operation and planning. Controlling modern power systems has become very difficult due to increased demand and consequential increase in power flow. Voltage stability is the ability of a power system to maintain acceptable voltages at all buses in the system under normal operating conditions (Steady State conditions) and/or after being subjected to a disturbance[24][25].

In power system operation and planning, voltage stability is now one of the main concerns to maintain system security. A system is said to have entered a state of voltage instability when a disturbance, increase in load demand, or a change in system condition causes a progressive and uncontrollable drop in voltage occurring due to the inability of the network to meet the increase in demand for reactive power. Voltage instability is the cause of system collapse, wherein the system voltage decays to a level from which it is unable to recover. Several large-scale power system blackouts in the recent past all over the globe have been the consequence of instability characterized by voltage collapse phenomena. Hence, a proper analysis of voltage stability is essential for the successful operation and planning of the power system[26][1]. The causes of voltage stability problems are

- High reactive power consumption at load centers
- Generating stations located far from load centers
- Difficulties in the transmission of reactive power under heavy loads
- Due to improper locations of FACTS controllers

- Poor coordination between multiple FACTS controllers

The voltage instability has the following effects on the power system

- Loss of load in specific areas
- Tripping of transmission lines
- Voltage collapse in the system

Voltage stability can be improved using any of the following.

- Placement of FACTS controllers
- Co-ordination of multiple FACTS controllers
- Installation of synchronous condensers
- Placement of series and shunt capacitors/reactors

3.5 Overview of FACTS

The development of FACTS devices has started with the growing capabilities of power electronic components. Devices for high power levels have been made available in converters for high and even highest voltage levels. The overall starting points are network elements influencing the reactive power or the impedance of a part of the power system[27]. In Figure 3.1 shows a number of basic devices separated into the conventional ones and the FACTS-devices. The left column contains the conventional devices build out of fixed or mechanically switchable components like resistance, inductance or capacitance together with transformers. The FACTS-devices contain these elements as well but use additional power electronic valves or converters to switch the elements in smaller steps or with switching patterns within a cycle of the alternating current. The right column of FACTS-devices uses Thyristor valves or converters. These valves or converters are well known for several years. They have low losses because of their low switching frequency of once a cycle in the converters or the usage of the Thyristor s to simply bridge impedances in the valves. Several FACTS-devices have been introduced for various applications worldwide. A number of new types of devices are in the stage of being introduced in practice. In most of the applications the controllability is used to avoid cost-intensive or landscape requiring extensions of power systems, for instance like upgrades or additions of substations and power lines[28][29].

FACTS-devices provide a better adaptation to varying operational conditions and

improve the usage of existing installations.

The basic applications of FACTS-devices are:

- Power flow control.
- Increase of transmission capability.
- Voltage control.
- Reactive power compensation.
- Stability improvement.
- Power quality improvement.
- Power conditioning.
- Flicker mitigation.
- Interconnection of renewable and distributed generation

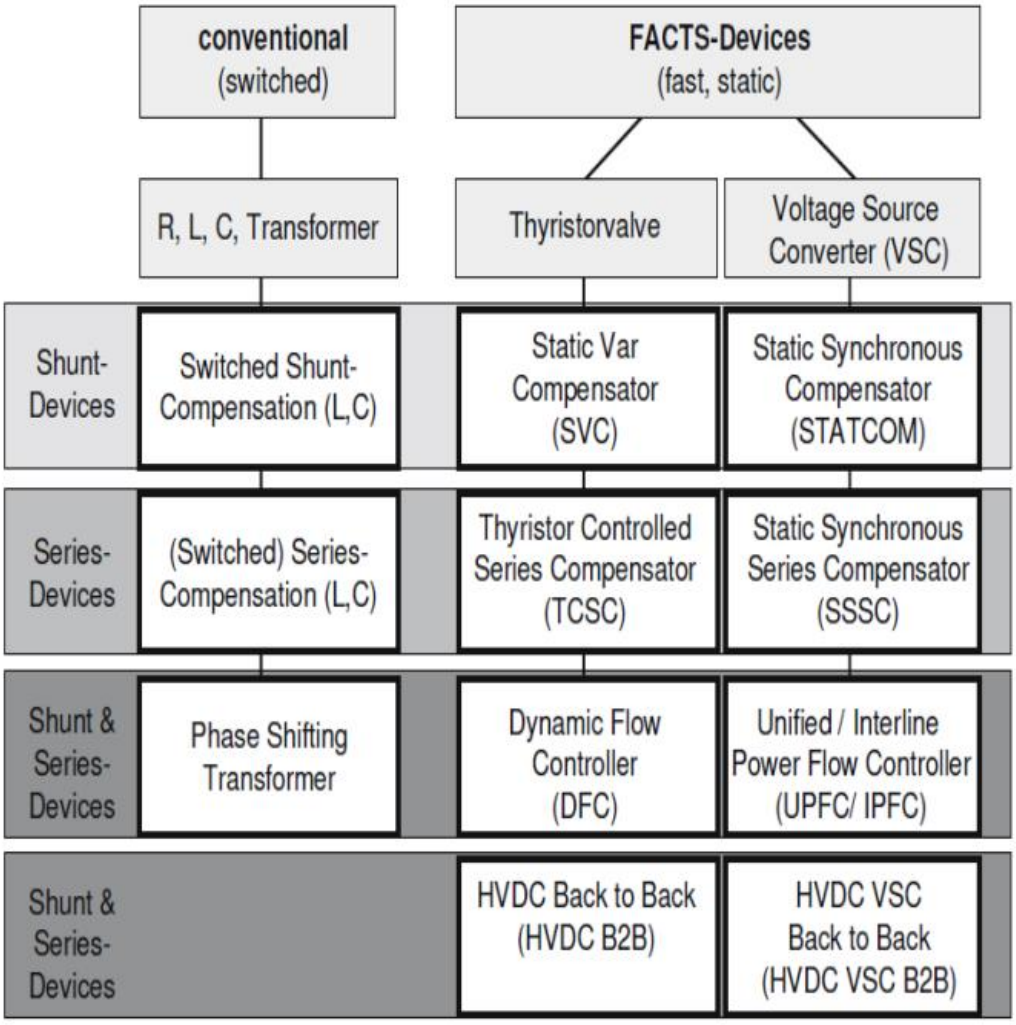

Figure 3.1: Overview of FACT devices[27]

3.6 Distribution Static Synchronous Compensator

D-STATCOM or a distribution Static Synchronous Compensator is a shunt device, which uses force-commutated power electronics (i.e. GTO, IGBT) to control power flow and improve transient stability on electrical power networks. It is also a member of the so-called Flexible AC Transmission System (FACTS) devices. The D-STATCOM is a three-phase shunt connected Voltage Source Converter (VSC) designed for use in the distribution network to compensate for the bus voltage so as to provide better power factor and reactive power. The device is capable of injecting or absorbing both active and reactive current at the point of common coupling (PCC). The limit constraint attached to energy storage makes it practically impossible for D-STATCOM to inject active power over a long period of time. Thus, the operation is mostly in steady-state with reactive power being the power exchange between D-STATCOM and the system. A typical model of D-STATCOM for steady-state operation consists of a coupling transformer with a leakage reactance, a GTO/IGBT, voltage source converter (VSC) and a DC capacitor. Figure 3.2 shows a schematic diagram of D-STATCOM incorporated to a bus k [30].

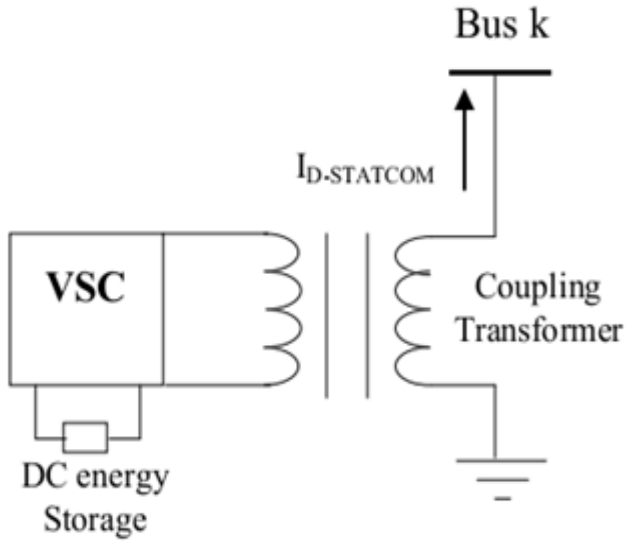

Figure 3.2: Statcom connected to a certain bus k[31]

Figure 3.3: A 1250 KVAr D-STATCOM unit [54]

3.6.1 Components of D-STATCOM

D-STATCOM consists of a three-phase inverter (generally a PWM inverter) using SCRs, MOSFETs or IGBTs, a D.C capacitor which provides the D.C voltage for the inverter, a link reactor which links the inverter output to the AC supply side, filter components to filter out the high-frequency components due to the PWM inverter. From the DC Side capacitor, a three-phase voltage is generated by the inverter. This is synchronized with the AC supply. The link inductor links system voltage to the AC supply side.

3.6.2 Basic Operating Principle of D-STATCOM

D-STATCOM operates in a similar manner as the synchronous machine, providing lagging current when under excited and leading current when overexcited. The voltage of D-STATCOM is injected in phase with the line voltage and in this case, there is no exchange of energy with the network, but only reactive power is to be injected (or absorbed) by the D-STATCOM as shown in Figure 3.2. The reactive power exchange with the network is achieved by varying the amplitude of the output voltages.

The output voltage of the Vsc is controlled in phase with the system voltage Vs. If Vvsc

is greater than Vs then D-STATCOM will act as a capacitor and generates reactive power (Capacitive mode). On the other hand, if Vs is greater Vvsc then the D-STATCOM will act as an inductor and consume reactive power (Inductive mode). If Vvsc is equal to Vs then D-STATCOM does not generate or absorbs reactive power and the reactive power is zero (No-load mode). The three operating modes of D-STATCOMS are shown in Figure 3.4 below:

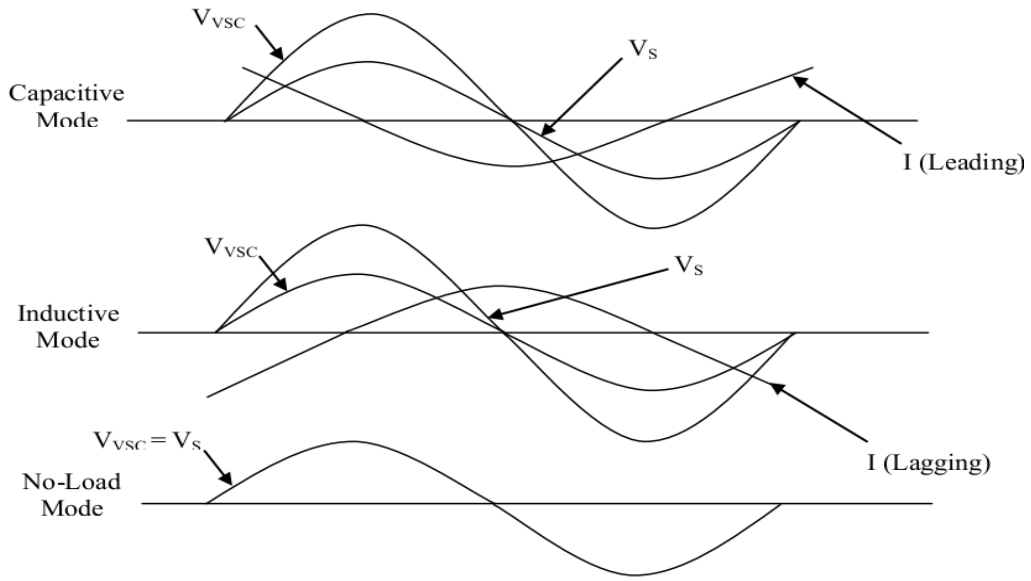

Figure 3.4: Operating Modes of D-STATCOM[27]

3.6.3 Applications of D-STATCOM

D-STATCOMs are typically applied in long-distance transmission systems, power substations and heavy industries where voltage stability is the primary concern. In addition; static synchronous compensators are installed at selected points in the power system to perform the following basic functions[32]:
The basic functions of D-STATCOM include:

1. Voltage regulation and reactive power compensation
2. Compensation of harmonic currents
3. Correction of the power factor
4. Mitigation of voltage flicker
5. Uninterrupted supply in case of use as an energy storage device

3.6.4 Reasons for choosing D-STATCOM

Providing power demand to the entire load by maintaining voltage magnitude at an acceptable range is one of the major system constraints in the distribution system. There are two principal conventional means of controlling voltage on distribution systems: Series voltage regulator and shunt capacitors are the two conventional ways of maintaining voltages of the distribution system at an acceptable range, but these devices have some disadvantages that are conventional series voltage regulators cannot generate reactive power and have quite slow response because of their step by step operations. The disadvantage with the shunt capacitors is that they cannot generate continuously variable reactive power and their natural oscillatory behavior when they are used in the same circuit with inductive components[33][34].

The reason for D-STATCOM is chosen as a compensating device as compared with other shunt FACTS equipment's are:

- autonomously control the voltage resulting in a much faster power factor correction
- continuously variable output without steps, no harmonics, no transients
- It can generate and absorb reactive power.
- Reacts practically instantaneously. The reaction starts <10ms after the event, full power result in 20-50ms
- is always in "hot standby", power losses <1%
- will work on a system near the stability limit

3.7 Modeling of D-STATCOM

The steady state mathematical modeling of D-STACOM is explained as follows, a simple two bus radial distribution system is shown below in Figure 3.5[9][10].

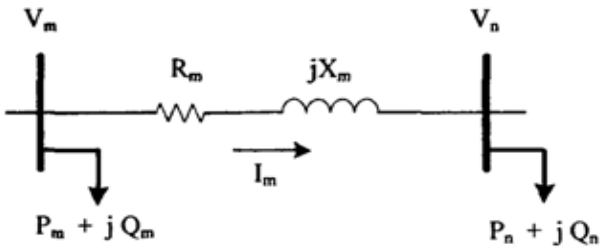

Figure 3.5: Two bus radial distribution system

The voltage equation for the two bus system is given as follows

$$V_n = V_m \angle \theta_m - (R_m + jX_m) I_m \angle \delta \quad (3.1)$$

For steady state modeling of D-STATCOM, it is installed at the bus as shown in Figure 3.6.

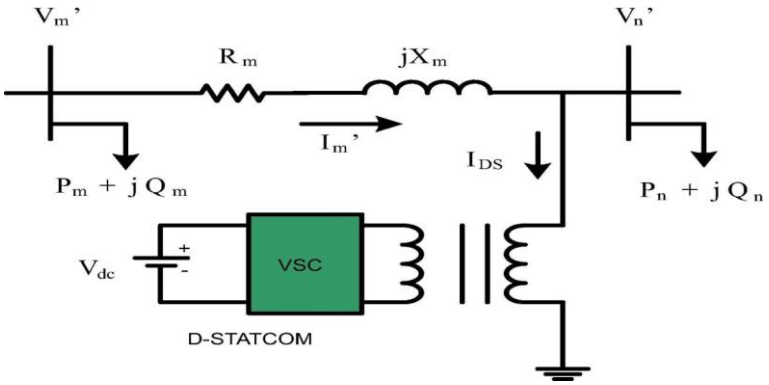

Figure 3.6: Two bus radial distribution system with D-STATCOM[31]

By installing D-STATCOM, the voltage values at the bus where it is installed and at the neighboring bus changes. The new voltages are $V_n^{'}$ at the candidate bus and $V_m^{'}$ at previous neighboring buses changes. The current changes to $I_m^{'}$ which is the summation of I_m and I_{DS}. Here I_{DS} is the current injected by D-STATCOM and is in quadrature with voltage. Therefore the expression for new voltage after installing D-STATCOM is given as

$$V_n^{'} \angle \theta_n = V_m^{'} \angle \theta_m^{'} - (R_m + jX_m)(I_m \angle \delta + I_{DS} \angle (\frac{\pi}{2} + \theta_n^{'})) \quad (3.2)$$

Here $\theta_n^{'}$, $\theta_m^{'}$, and δ are the phase angles of $V_n^{'}, V_m^{'}$ and I_m respectively.

On separating real and imaginary parts of the above equations, we get

$$V_n^{'} \cos\theta_n^{'} = \mathrm{Re}\,al(V_m^{'} \angle \theta_m^{'}) - \mathrm{Re}\,al(Z_m I_m \angle \delta) - R_m I_{DS} \cos(\frac{\pi}{2} + \theta_n^{'}) + X_m I_{DS} \sin(\frac{\pi}{2} + \theta_n^{'}) \quad (3.3)$$

$$V_n^{'} \sin\theta_n^{'} = \mathrm{Im}\,ag(V_m^{'} \angle \theta_m^{'}) - \mathrm{Im}\,ag(Z_m I_m \angle \delta) - X_m I_{DS} \cos(\frac{\pi}{2} + \theta_n^{'}) + R_m I_{DS} \sin(\frac{\pi}{2} + \theta_n^{'}) \quad (3.4)$$

Now by taking some assumptions

$V_n^{'}$=b

$h1 = \mathrm{Re}\,al(V_m^{'} \angle \theta_m^{'}) - \mathrm{Re}\,al(Z_m I_m \angle \delta)$

$h2 = \mathrm{Im}\,ag(V_m^{'} \angle \theta_m^{'}) - \mathrm{Im}\,ag(Z_m I_m \angle \delta)$

$h3 = -X_m$

$h4 = -R_m$

I_{DS} =x1

$\theta_n^{'}$ = x2

So equations (3.3) and (3.4) changes to

$$b\cos x_2 = h_1 - h_4 x_1 \sin x_2 - h_3 x_1 \cos x_2 \quad (3.5)$$

$$b\sin x_2 = h_2 - h_3 x_1 \sin x_2 - h_4 x_1 \cos x_2 \quad (3.6)$$

So from equation (3.5) $x_1 = \dfrac{b\cos x_2 - h_1}{-h_4 \sin x_2 - h_3 \cos x_2}$ (3. 7)

And from equation (3.6) $x_1 = \dfrac{b\sin x_2 - h_2}{-h_3 \sin x_2 - h_4 \cos x_2}$ (3. 8)

By equating both equations (3.7) and (3.8), we get

$$\frac{b\cos x_2 - h_1}{-h_4 \sin x_2 - h_3 \cos x_2} = \frac{b\sin x_2 - h_2}{-h_3 \sin x_2 - h_4 \cos x_2}$$

On cross multiplying we get

$$bh_4 + (h_1 h_3 - h_2 h_4)\sin x_2 + (-h_1 h_4 - h_2 h_3)\cos x_2 = 0 \quad (3.9)$$

Let

$\sin x_2$ =t (3. 10)

$(h_1 h_3 - h_2 h_4)$ =k1 (3. 11)

$(h_1 h_4 + h_2 h_3)$ =k2 (3. 12)

So equation (3.9) changes to

$$bh_4 + k_1 t - k_2\sqrt{1-t^2} = 0 \quad (3.13)$$

$$bh_4 + k_1 t = k_2\sqrt{1-t^2} \quad (3.14)$$

On squaring both sides and manipulating, we get

$$(k_1^2 + k_2^2)t^2 + 2bh_4 k_1 t + b^2 h_4^2 - k_2^2 = 0 \quad (3.15)$$

This gives

$$t = \frac{-B \pm \sqrt{D}}{2A} \quad (3.16)$$

$$D = B^2 - 4AC \quad (3.17)$$

Where

$$A = K_1^2 + K_2^2 \quad (3.18)$$

$$B = 2bh_4K_1 \tag{3. 19}$$

$$C = b^2h_4^2 - k_2^2 \tag{3. 20}$$

On putting values of K_1 and K_2 we get,

$$A = (h_1h_3 - h_2h_4)^2 + (h_1h_4 + h_2h_3)^2 \tag{3. 21}$$

$$B = 2(h_1h_3 - h_2h_4) + (V_n^{'})(h_4) \tag{3. 22}$$

$$C = (V_n^{'}.R_m)^2 - (h_1h_4 + h_2h_3)^2 \tag{3. 23}$$

Now there are two roots of t. For determining the correct value of root, the boundary considerations are examined $V_n^{'} = V_n \Rightarrow I_{DS} = 0$ and $\theta_n^{'} = \theta_n$

Results show that $t = \dfrac{-B \pm \sqrt{D}}{2A}$ is the correct root of an equation

Thus the bus voltage phase angle is

$$\theta_n^{'} = \sin^{-1}\left(\frac{-B \pm \sqrt{D}}{2A}\right) \tag{3. 24}$$

D-STATCOM current angle and magnitude is:

$$\angle I_{DS} = \frac{\pi}{2} + x_2 = \frac{\pi}{2} + \sin^{-1} t \tag{3. 25}$$

$$\left|I_{DS}\right| = x_1 = \frac{V_n^{'}\cos\theta_n - h_1}{-h4\sin\theta_n^{'} - h3\cos\theta_n^{'}} \tag{3. 26}$$

Finally, the reactive power injected is:

$$jQ_{DS} = (V_n^{'}\angle\theta_n^{'}).(I_{DS}\angle(\frac{\pi}{2} + \theta_n^{'}))^* \tag{3. 27}$$

Where * denotes the complex conjugate.

3.8 Power flow analysis

Load flow studies use to ensure that electrical power transfer from generators to consumers through the grid system is stable, reliable, and economic. The main characteristics of radial distribution feeders are the radial structure, the multi-phase conductors, the unbalanced load operation and their high R/X ratio. These features may cause traditional power flow methods such as Conventional Gauss-Seidel, Newton-Rapson, and Fast Decoupled Load Flow algorithms to return poor convergence characteristics and fail in meeting the distribution system requirements[35][36].

In the same connection, it is often possible to have the primary distribution feeder and

all of its laterals consist of a 3-phase system. Such being the case, some power companies may consider the feeder operates in a balanced load condition.

Alternatively, suitable power flow methods specially designed for radial distribution systems are used. The backward/forward sweep and the ladder iterative methods are among the potential methods. The basic principle of each is similar, where the voltage magnitude and phase angle of the source should be specified. Also, the complex values of load demands at each node along the feeder should be given. Starting from the end of the feeder, the backward sweep calculates the line section currents and node voltages (by KCL and KVL) back to the source. The calculated voltage at the source is compared with its original specified value. If the error is beyond the limit the forward sweep is performed to update the node voltages along the feeder. In such a case, the specified source voltage and the line section currents already calculated in the previous backward sweep are used. The process keeps going back and forth until the voltage error at the source becomes within the limit.

3.8.1 Forward / Backward Sweep load flow method

Forward/backward sweep-based power flow algorithms generally take advantage of the radial network topology and consist of forward and/or backward sweep processes. The forward sweep is mainly the node voltage calculation from the sending end to the far end of the feeder and laterals, and the backward sweep is primarily the branch current and/or power summation from the far end to the sending end of the feeder and laterals. In some algorithms in addition to the branch current and/or power summation, the node voltages are also computed in backward sweep[10].

The algorithm is developed based on two derived matrices, the bus-injection to the branch-current matrix and the branch current to the bus-voltage matrix, and equivalent current injections. For distribution networks, the equivalent current-injection based model is more practical. For the bus, the complex load S_i is expressed by:

$$S_{Li} = P_{Li} + jQ_{Li} \qquad (3.\ 28)$$

Where $i=1 \ldots N$

Step-1: Backward Sweep

For each iteration k, branch currents are aggregated from loads to the origin. But before finding the branch current we need to find the current injected at each bus and the bus-injection to branch-current (BIBC) which relates the bus injected current to the branch current. The current injection at the k[th] iteration of the i[th] bus is

$$I_i^k = I_i^r\ (V_i^k) + jI_i^i\ (V_i^k) = \left(\frac{P_i + jQ_i}{V_i^k} \right) \qquad (3.29)$$

Where V_i^k and I_i^k are the bus voltage and equivalent current injection of i[th] bus at k [th] iteration, respectively. I_i^r and I_i^i are the real and imaginary parts of the equivalent current injection of bus i at the K[th] iteration, respectively.

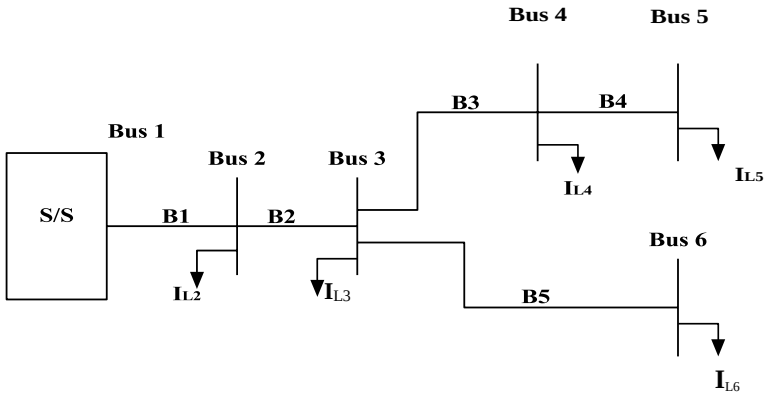

Figure 3.7: Sample distribution system

From Equation 3.29, injected currents are obtained. By applying Kirchhoff's current law (KCL) to the distribution network, the branches current are calculated. Simple distribution system, shown in Figure 3.7, is used as a sample test system. Branch currents can then be formulated as functions of equivalent current injections. The branch currents B_2, B_3, B_4 and B_5 can be expressed as:

$B_1 = I2 + I3 + I4 + I5 + I6$

$B_2 = I3 + I4 + I5 + I6$

$B_3 = I4 + I5$

$B_4 = I5$

$B_5 = I6$

Therefore, the relationship between the bus current injections and branch currents can be expressed by:

$$\begin{pmatrix} B1 \\ B2 \\ B3 \\ B4 \\ B5 \end{pmatrix} = \begin{bmatrix} 1 & 1 & 1 & 1 & 1 \\ 0 & 1 & 1 & 1 & 1 \\ 0 & 0 & 1 & 1 & 0 \\ 0 & 0 & 0 & 1 & 0 \\ 0 & 0 & 0 & 0 & 1 \end{bmatrix} \begin{bmatrix} I2 \\ I3 \\ I4 \\ I5 \\ I6 \end{bmatrix} \quad (3.30)$$

Where: BIBC is a bus injection to branch current matrix, which is the upper triangular matrix and contains values of zero and one only in Equation 3.30.

Step-2: Forward sweep

Nodal voltage vector V is updated from the origin to loads according to the Kirchhoff Voltage Laws (KVL), using previously calculated branch currents vector B and branch-current to bus-voltage (BCBV). The relationship between branch currents and bus voltages as shown in Figure 3.7 can be expressed as:

$$V_2 = V_1 - B_1 Z_{12}$$
$$V_3 = V_2 - B_2 Z_{23} = V_1 - B_1 Z_{12} - B_2 Z_{23}$$
$$V_4 = V_3 - B_3 Z_{34} = V_1 - B_1 Z_{12} - B_2 Z_{23} - B_3 Z_{34}$$
$$V_5 = V_4 - B_4 Z_{45} = V_1 - B_1 Z_{12} - B_2 Z_{23} - B_3 Z_{34} - B_4 Z_{45}$$
$$V_6 = V_3 - B_5 Z_{56} = V_1 - B_1 Z_{12} - B_2 Z_{23} - B_5 Z_{56}$$

Where: - V_i is the voltage of bus i, and

Z_{ij} is the line impedance between bus i and bus j

From Equation 3.31, it can be seen that the bus voltage can be expressed as a function of branch currents, line parameters, and the substation voltage. Similar procedures can be performed on other buses; therefore, the relationship between branch currents and bus voltages can be expressed as:

$$\begin{bmatrix} V1 \\ V2 \\ V3 \\ V4 \\ V5 \end{bmatrix} = \begin{bmatrix} V1 \\ V1 \\ V1 \\ V1 \\ V1 \end{bmatrix} \begin{bmatrix} Z12 & 0 & 0 & 0 & 0 \\ Z12 & Z23 & 0 & 0 & 0 \\ Z12 & Z23 & Z34 & 0 & 0 \\ Z12 & Z23 & Z34 & 0 & 0 \\ Z12 & Z23 & 0 & 0 & Z56 \end{bmatrix} \begin{bmatrix} B1 \\ B2 \\ B3 \\ B4 \\ B5 \end{bmatrix} \quad (3.31)$$

Where

BCBV is the branch current to bus voltage which is given by for the given sample network

$$[BCBV] = \begin{bmatrix} Z12 & 0 & 0 & 0 & 0 \\ Z12 & Z23 & 0 & 0 & 0 \\ Z12 & Z23 & Z34 & 0 & 0 \\ Z12 & Z23 & Z34 & Z45 & 0 \\ Z12 & Z23 & 0 & 0 & 0 \end{bmatrix} \quad (3.\ 32)$$

The general form for the bus voltage at (k+1) th iteration can be expressed as

$$\left[V^{k+1}\right] = [V_1] - [BCBV][B] \quad (3.\ 33)$$

In general form, with i and k denoting the node and iteration number respectively,

$$I^K_{i-1,i} = I^k_i + I^k_{i,i+1} \quad (3.\ 34)$$

$$V^k_i = V^k_{i-1} - Z_{i-1,i} * I^{k-1}_{I-1,I} \quad (3.\ 35)$$

3.8.1.1 Procedure Forming BIBC and BCBV Matrix

As seen above the BIBC and BCBV matrices are developed based on the topological structure of distribution systems. The BIBC matrix represents the relationship between bus current injections and branch currents. The corresponding variations at branch currents, generated by the variations at bus current injections, can be calculated directly by the BIBC matrix.

The BCBV matrix represents the relationship between branch currents and bus voltages. The corresponding variations at bus voltages, generated by the variations at branch currents, can be calculated directly by the BCBV matrix. So the procedures for forming the BIBC and BCBV are shown below:

Procedure 1: Forming BIBC

Step 1: For a distribution system with the m-branch section and n-bus, the dimension of the BIBC matrix is m x (n-1).

Step 2: If a line section (B_k) is located between bus i and bus j, copy the column of the i-th bus of the BIBC matrix to the column of the j-th bus and fill a 1 to the position of the k-th row and the j-th bus column.

Step 3: Repeat step (2) until all line sections are included in the BIBC matrix.

Procedure 2: Forming BCBV

Step 1: For a distribution system with the m-branch section and n-bus, the dimension of the BCBV matrix is (n-1) × m.

Step 2: If a line section is located between bus i and bus j, copy the row of the i^{th} bus of the BCBV matrix to the column of the j-th bus and fill the line impedance (Zij) to the position of the k-th column and the j-th bus row.

Step 3: Repeat step (2) until all line sections are included in the BCBV matrix.

3.8.1.2 Power loss and voltage drop calculation

Reducing the losses is a major objective of any electrical utility because if they exceed certain allowable levels, they can actually endanger the company's financial status. Of course, the losses concern the entire power systems, from production through the transmission to distribution; but the discussion is mostly oriented toward losses in the distribution networks, where most of them occur. Losses in electrical power distribution systems include technical and non-technical losses.

The technical losses are related to the energy distribution process that happens because of the physical nature of the equipment and infrastructure of the power systems, i.e. and copper loss in conductor cables, transformer switches, and generators. The non-technical losses are related to the customer management process incorrect operation of the meters and illegal use in collaboration with utility personnel.

Power loss calculation

The line losses can be calculated in the distribution system in both primary and secondary feeders. [37].The active and reactive power loss in the distribution system per phase can be calculated as following:

$$P_{loss} = \sum_{i=1}^{nb} |I(i)|^2 * R(i) \quad (3.\ 36)$$

$$Q_{loss} = \sum_{i=1}^{nb} |I(i)|^2 * X(i) \quad (3.\ 37)$$

The total active and reactive power loss of the distribution systems is found by adding each branch current line losses:

$$P_{TLoss} = \sum_{t=1}^{nb} P_{Loss(t,t+1)} \quad (3.38)$$

Voltage Drop Calculation

All equipment connected to the utility system is designed to be used in a certain definite voltage. It is not practical, to serve every customer on a power distribution at the same voltage corresponding exactly to the name plate voltage because the voltage drops exist in each part of the power system from generating to the customer's meter[38].

Voltage drop in the distribution system can be calculated as:

$$\Delta V = \sqrt{3} \times \sum_{i=1}^{n} I_i (R_i \cos\theta + X_i \sin\theta) L_i \qquad (3.\ 39)$$

Where

I_i	Portion current on line (A)
θ	Angle between current and voltage
R_i	Resistance of the line (Ohm/km)
X_i	Reactance of the line (Ohm/km)
n	Number of portions
L_i	Portion length of the line (km)

3.9 Particle swarm optimization

Particle Swarm Optimization (PSO) is evolutionary programming and it is a latest population-based optimization method that was introduced by James Kennedy & Russell Eberhart in 1995 for optimizing continuous nonlinear functions[39].

PSO takes its inspiration from the behavior of birds, fishes, insects and their communities. They manage as a group, rather than as individuals, recreating themselves and adapting in accordance with the changes in the surrounding environment, in order to search for food or to migrate. In other words, PSO is mainly inspired by social behavior patterns of organisms that live and interact within a large group and the members of the entire population are maintained through the search process[40].

Figure 3.8: School of fishes [52]

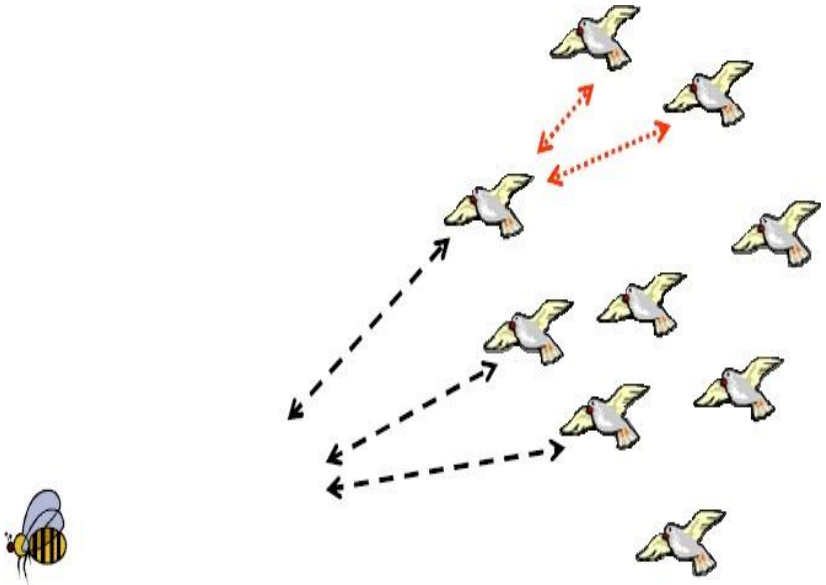

Figure 3.9: Flock of birds [52]

The PSO algorithm starts with a population of particles with random positions in the search space. Each particle is a solution to the problem and has a fitness value. The fitness is evaluated and is to be optimized. Velocity is defined which directs each particle's position and gets updated in each iteration. Particles gradually move toward the optimal due to their best position they have ever experienced and the best solution which group has experienced. The velocity of a particle is updated due to three factors: the past velocity of the particle, the best position particle has experienced so far and the best position the entire swarm has experienced so far as shown in Figure 3.10 & 3.11

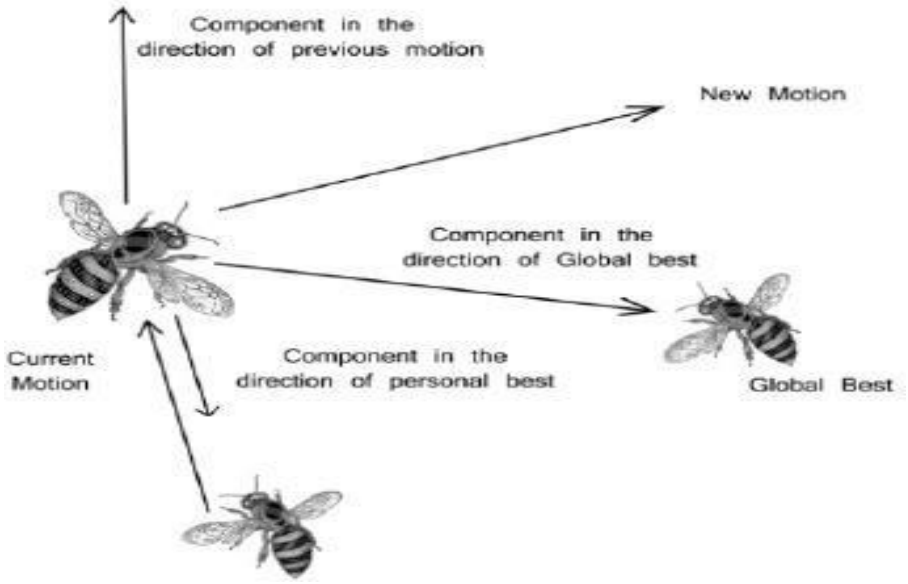

Figure 3.10: Concept of a searching point by PSO [52]

PSO algorithm is one of the most powerful and recent methods for solving the non-smooth global optimization problems. Some of the advantages of PSO are the following[41]:

- It is efficient in the global search and derivative-free algorithm.
- It is easy to perform and conceptually very simple, so it can be applied both in scientific research and engineering problems.
- It has a limited number of parameters and the impact of parameters on the solutions is small compared to other optimization techniques.
- PSO uses probabilistic transition rules and not deterministic rules. Hence, PSO is a kind of stochastic optimization algorithm that can search for a complicated and uncertain area.
- Unlike the Genetic Algorithm (GA) and other heuristic algorithms, PSO has the flexibility to control the balance between the global and local exploration of the search space. This unique feature of a PSO overcomes the premature convergence problem and enhances the search capability.
- Unlike the traditional methods, the solution quality of the proposed approach doesn't rely on the initial population.

- Starting anywhere in the search space, the algorithm ensures the convergence to the optimal solution.
- PSO is a population-based search algorithm (i.e., PSO has implicit parallelism). This property ensures PSO to be less susceptible to getting trapped on local minima.
- PSO uses payoff (performance index or objective function) information to guide the search in the problem space. Therefore, PSO can easily deal with non-differentiable objective functions. Additionally, this property relieves PSO of assumptions and approximations, which are often required by traditional optimization models.

The only major disadvantages of PSO are;

- The method easily suffers from partial optimism, which causes the less exact at the regulation of its speed and direction.
- The method may not work out properly the problems of the non-coordinate system, such as the solution to the energy field and the moving rules of the particles in the energy field.

Mathematical expression

Mathematically the modification process may be expressed as follows[42]:

$$V_{id}^{k+1} = wV_{id}^{k} + c_1 r(P_{bestid} - S_{id}^{k}) + c_2 r(G_{bestid} - S_{id}^{k}) \quad (3.40)$$

$$S_{id}^{k+1} = S_{id}^{k} + V_{id}^{k+1} \quad (3.41)$$

$$; i=1, 2\ldots n \;\&\; d=1, 2\ldots m$$

Where

V_{id}^{k+1}	is the modified velocity of agent i
w	is weight function for a velocity of agent
V_{id}^{k}	is current velocity
P_{bestid}	is the particles best position
c_1 and c_2	are weight coefficients for each term respectively
S_{id}^{k}	is the current searching point

S_{id}^{k+1}	is the modified searching point
G_{bestid}	is the group best position
n	is the number of particles in a group
m	is the number of members in the particle
r	is a random number

The following weight function is used

$$W_K = W_{\max} - \left(\frac{W_{\max} - W_{\min}}{K_{\max}} \right).k \qquad (3.\ 42)$$

Where, $W_{\min}$ and $W_{\max}$ are the minimum and maximum weights respectively.

K and K_{max} are the current and maximum iteration.

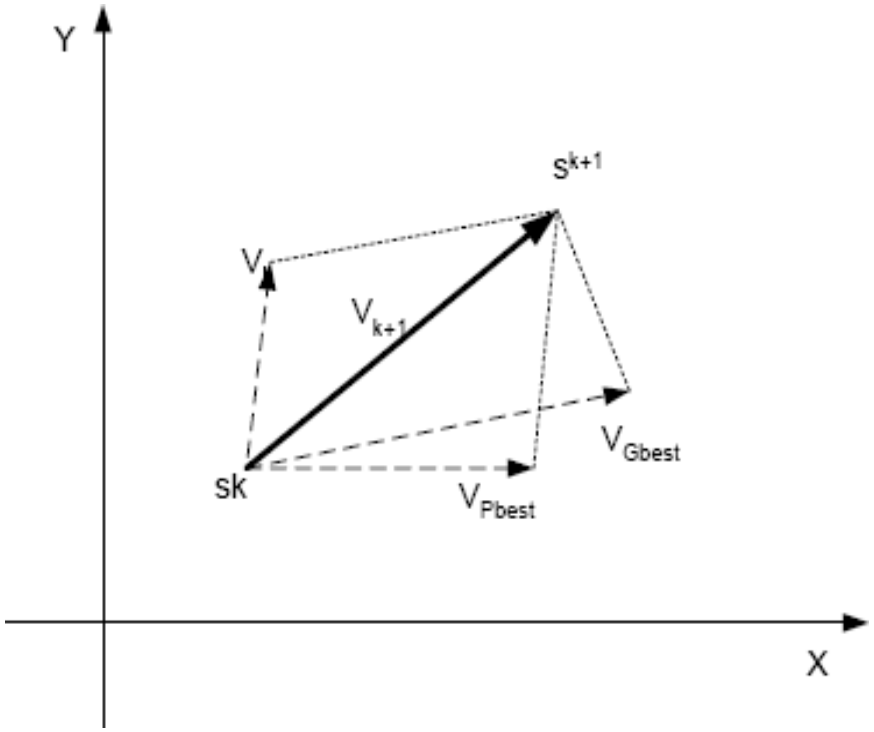

Figure 3.11: Velocity updating in PSO

3.9.1 Choice of PSO Parameters

The most important parameters in the PSO algorithm include[43][44]:

Population: it is a set of x particles at time t.

Swarm: it is an apparently disorganized population of moving particles that tend to cluster together while each particle seems to be moving in a random direction.

Individual best: As the particle moves through the search space, it compares its fitness value at the current position to the best fitness value it has ever attained at any time up to the current time. The best position that is associated with the best fitness encountered so far is called the individual best for each particle in the swarm, can be determined and updated during the search.

Global best: It is the best position among all of the individual best positions achieved so far.

Particle Velocity: The current velocity V_{id}^{k} is constrained in the limits $V_{id}^{\min} \le V_{id}^{k} \le V_{id}^{\max}$

The parameter $V^{\max}$ determines the resolution, or fitness, showing which regions are to be searched between the present position and the target position. If $V^{\max}$ is very high; particles might fly past good solutions. This is because the particles move in larger steps and the solution reached may not optimal. Similarly if $V^{\max}$ is too small, particles take longer time to reach desired solutions. They may even not explore sufficiently hence being captured in local minimum solutions. In many experiences with PSO, $V^{\max}$ is often set at 12–25% of the dynamic range of the variable on each dimension.

Random Numbers: The uniform random values are in the range [0, 1]. They help in achieving the stochastic behavior of PSO.

Weighting Coefficients: The parameters c_1 and c_2 represent the weighting of the stochastic acceleration terms. High values result in abrupt movement toward, or past, target regions. On the other hand, low values allow particles to roam far from the target regions before being tugged back. The parameters c_1 and c_2 may be adopted in the range as the number of iterations increases, but in many applications c_1 and c_2 are often constants. c_1 and c_2 control the rate of the relative influence of the memory of other particles and their typical values are $c_1 = c_2 = 2$.

Inertia Weight: Suitable choice of the inertia weight can supply a balance between

global and local explorations. That is a balancing factor between exploration and exploitation. For faster convergence, inertia weight is usually selected to be high at the beginning and is decreased in the course of optimization. In general, the inertia weight w is adjusted according to equation 3.42 above. Appropriate values for $W_{\min}$ and $W_{\max}$ are 0.4 and 0.9 respectively.

Stopping criteria: These are the conditions under which the search process will terminate. In this study, the search will terminate if the maximum iteration is satisfied. The basic PSO described above has some number of parameters that need to be fixed. The first parameter is the size of the population. This is often set empirically on the basis of the dimensionality and perceived the difficulty of a problem. Values in the range 20–50 are quite common. The second parameters c_1 and c_2 in Equation 3.40 commonly called acceleration coefficients which determine the magnitude of the random forces in the direction of personal best and neighborhood best.

The behavior of a PSO changes radically with the value of c_1 and c_2. When $c_1=c_2=0$, then all particles continue flying at their current speed until they hit the search spaces boundary, When $c_1>0$ and $c_2=0$, all particles are independent on the other hand When $c_1=0$ and $c_2>0$ all particles are attracted to a single point in the entire swarm, when $c_1=c_2$, all particles are attracted towards the average of p_{best} and g_{best}, when $c_1>c_2$ each particle is more strongly influenced by its personal best position, resulting in excessive wandering on the contrary when $c_2>c_1$ then all particles are much more influenced by the global best position, which causes all particles to run prematurely to the optima. In all cases, the velocity update equation is changed. However, the value $c_1=c_2=2.0$, almost universally adopted in early PSO research. Iteration number also another parameter of the PSO algorithm which is important to get a better result. A too low number of iterations may stop the search process prematurely, while too large iterations have the consequence of unnecessary added computational complexity and more time needed.

3.9.2 PSO Implementation Steps

In the PSO algorithm, the population has n particles that represent candidate solutions. Each particle is an m dimensional real-valued vector where m is the number of optimized parameters. Therefore each optimized parameter represents a dimension of the problem space[45].The proposed PSO technique for the optimization algorithm described using the following steps and shown in Figure 3.12.

Step 1**: Initialization**: Define all parameters and generate random n particles, each particle in the initial population is evaluated using the objective function f. Set the iteration counter k = 1. Randomly generates an initial population (array) of n particles. The initial velocity of each particle is randomly generated for the evaluation of the objective function. $K_{\max}$, $W_{\min}$, $W_{\max}$, c_1 and c_2 are assigned. In this Step, the lower and higher bound of regional constraints is specified too.

Step 2**: Objective function calculation**: Calculate the objective function and finds the fitness value of each particle.

Step 3**: Fitness value comparison**: The fitness value of each particle during the first iteration becomes its p_{best} . In preceding iteration if the new value of p_{best} is obtained well than previous then it's modified otherwise it's kept the same.

Step 4**: Assign the best personal best value as global best**: The best fitness value among all the p_{best} is denoted as G_{best} .

Step 5: **Velocity modification:** Modify the velocity of each particle using the following equation:

$$V_{id}^{k+1} = wV_{id}^{k} + c_1 r(P_{bestid} - S_{id}^{k}) + c_2 r(G_{bestid} - S_{id}^{k})$$

Then generate the new particles based on the following equation:

$S_{id}^{k+1} = S_{id}^{k} + V_{id}^{k+1}$; i=1, 2… n & d =1, 2..... m

Step 6: **Iteration updating**: Update the iteration counter, k = k+1.

Step 7: If stopping criteria is satisfied go to step 8 else go to step 2.

Step 8: Stop. The particle that generates at latest iteration is the optimal solution of PSO.

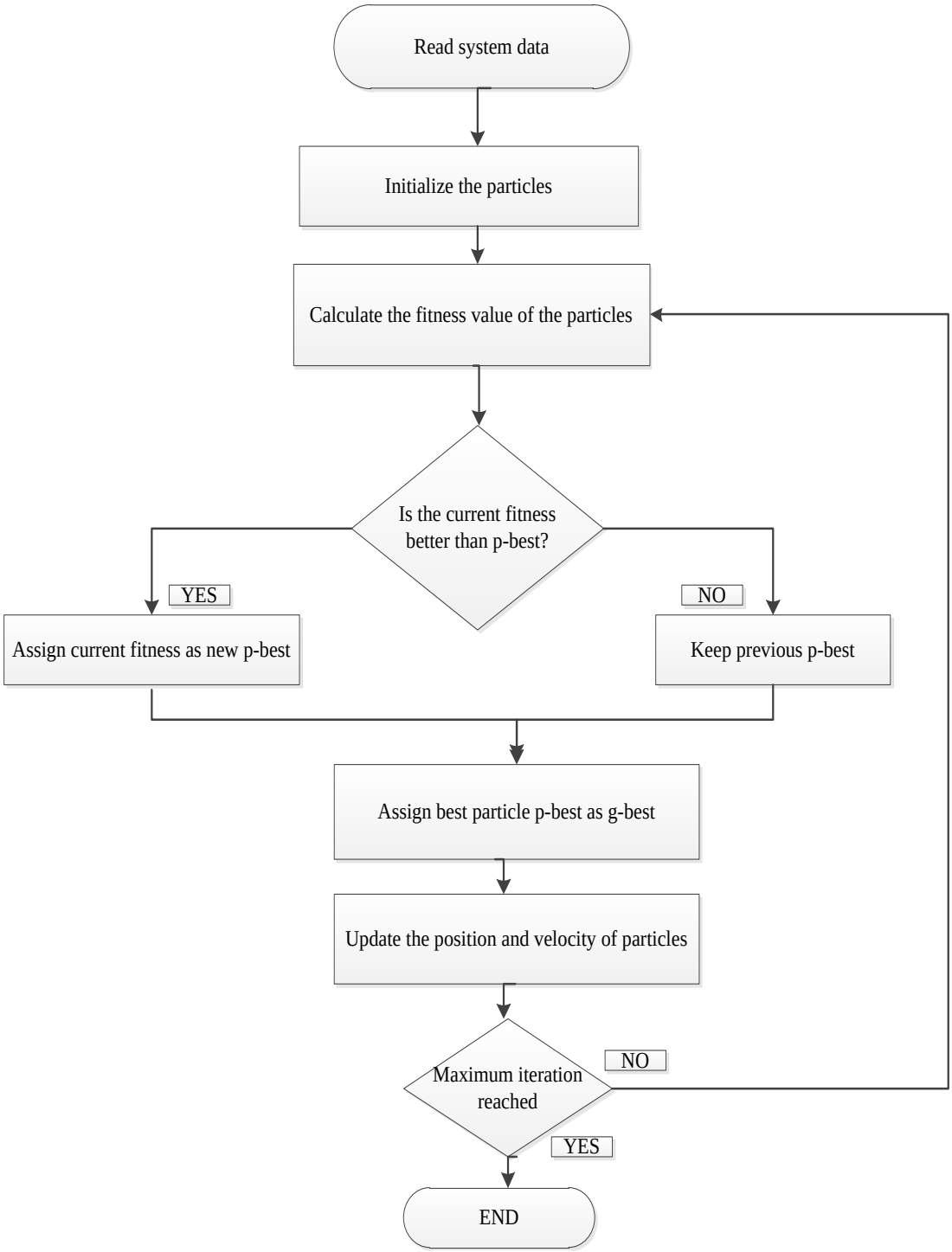

Figure 3.12: PSO flow chart

CHAPTER FOUR

4 METHODOLOGY

4.1 Distribution System Data Collection and Analysis

Bahir Dar is the capital city of Amhara National Regional State, which incorporates many industrial and commercial sectors. All the loads have fed from the two substations which are located at Bahir Dar city. The loads belonging to one segment have placed at the end of each segment. The layout diagram of Bahir Dar substation II as illustrated in Figure 4.1. The loads mainly supplied and interconnected from Tiss Abay I, Tiss Abay II, Beles and Fincha generation station and outgoing 230kV of Alamata and Gonder-Metema substation. There is one 400/230 kV substation (substation II), two 230/132/15kV and 230/66/15kV (substation II) transformer and one 66/45/15kV substation (substation I) transformer, which supplies the town. It consists of eleven radial feeders, of these Seven (Adet, Tis abay, Ghion, Papyrus, Industry, Bata and Airforce) feeders are from substation II and the rest four (Bete-mengist, Gambi, Hamusit and Boiler) feeders are from substation I.

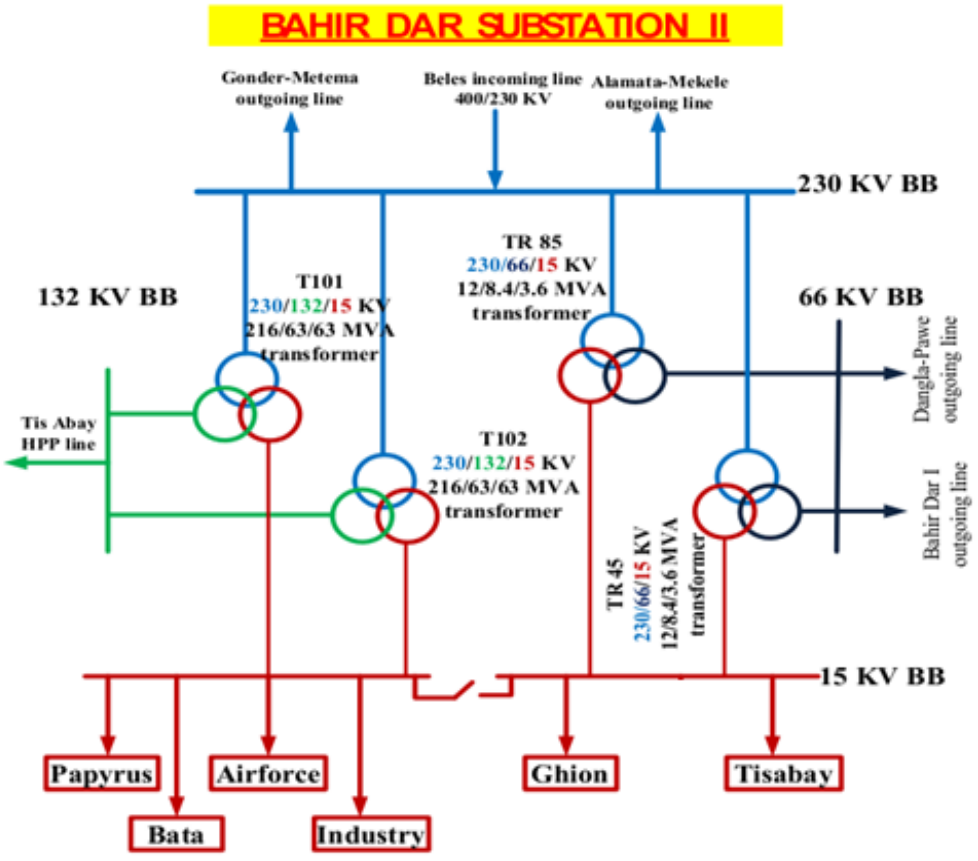

Figure 4.1: Single line diagram of Bahir Dar substation II

Among the seven 15KV outgoing feeders of Bahir Dar substation two, Papyrus feeder is selected for this case study the reasons are:

- High demand for power
- High peak load current
- Long distance covered

Papyrus feeder has 59 nodes, 58 segments, 47 loads, and a total capacity of 3.9 MW Single line diagram of papyrus feeder is shown in Figure 4.2 below

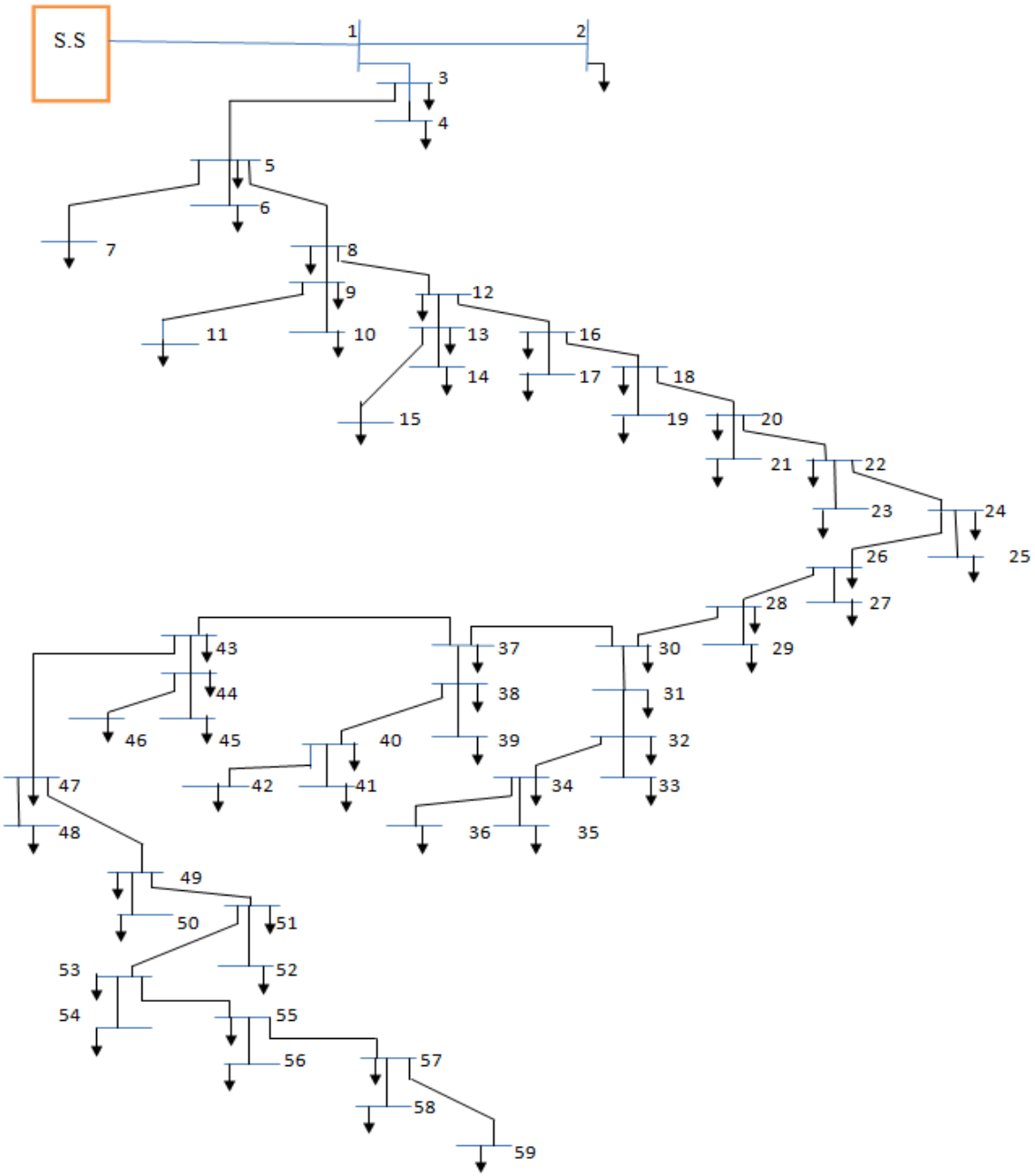

Figure 4.2: Single line diagram of papyrus feeder

4.1.1 Impedance Calculation of Overhead Line

The inductance of a transmission line depends upon the material, dimensions, and configuration of the wires and length with the spacing between them. AC resistance of a conductor is always higher than its DC resistance due to the skin effect forcing more current flow near the outer surface of the conductor. The higher the frequency of the current, the more noticeable the skin effect would be. Wire manufacturers usually supply tables of resistance per unit length at common frequencies (50 and 60 Hz). The conductors that are used in distribution feeders are stranded conductors. The inductive reactance is calculated at a frequency of 50Hz, and at a length of one kilometer. Thus, impedances are given by[46][47]:

$$Z_a = R_a + j0.06283 \ln \frac{D}{GMR_a} \Omega / km \quad (4.1)$$

$$GMR = k.r \quad (4.2)$$

$$D = \sqrt[3]{D_{ab}} D_{bc} D_{ac} \quad (4.3)$$

Where

GMR_a	Geometric mean ratio of conductor a
r	Actual conductor radius r
D	Distance between conductors in meter
D_{ab}	Distance between conductors a and b in meter
D_{bc}	Distance between conductors b and c in meter
D_{ac}	Distance between conductors a and c in meter
k	GMR factor
Z_a	Impedance of conductor a in Ω/km
R_a	Resistance of conductor i in Ω/km

1. For AAC-95 conductor type, the self-impedance for phase conductors is

$$Z_a = 0.3085 + j0.06283 \ln \frac{0.72135}{4.129 * 10^{-3}} \Omega / km \quad (4.4)$$
$$= 0.3085 + j0.32441 \Omega / km$$

For the three phases, three conductors the impedance of each conductor is the same (Za=Zb=Zc).Then the positive sequence impedance of the conductor is obtained by multiplying the impedance per kilometer by its length.

2. For AAC-50 conductor type

Using the same procedure as AAC-95 the process and equations are followed to obtain the impedance of the conductor for AAC-50. Thus, the positive sequence impedance is

$$Z_a = 0.3085 + j0.06283 \ln \frac{0.72135}{2.88*10^{-3}} \Omega / km \quad (4.5)$$
$$= 0.5785 + j0.3470 \Omega / k$$

For the three phases, three conductors the impedance of each conductor is the same (Za=Zb=Zc). Then the positive sequence impedance of the conductor is obtained by multiplying the impedance per kilometer by its length.

3. For AAC-25 conductor type

Using the same procedure as AAC-50 the process and equations are followed to obtain the impedance of the conductor for AAC-25. Thus, the positive sequence impedance is:

$$Z_a = 0.3085 + j0.06283 \ln \frac{0.72135}{1.881*10^{-3}} \Omega / km \quad (4.6)$$
$$= 1.181 + j0.3736 \Omega / km$$

For the three phases, three conductors the impedance of each conductor is the same (Za=Zb=Zc). Then the positive sequence impedance of the conductor is obtained by multiplying the impedance per kilometer by its length.

The GMR for each conductor is given in table 4.1.

Table 4.1 GMR Factor (k) and Strand Relationship for AAC conductor

Strands	GMR factor, k
1	0.7788
3	0.6778
7	0.7256
19	0.7577
37	0.7678
61	0.7722

Table 4.2: Conductor parameters in the feeder

Conductor type	Nominal area (mm^2)	Actual area (mm^2)	Stranding and wire diameter	Overall diameter (mm)	Actual diameter (mm)	GMR (mm)	Resistance (W/km)
AAC	25	24.2	7/2.1	6.3	5.56	1.88	1.181
AAC	50	49.5	7/3.00	9	7.9377	2.88	0.5785
AAC	95	93.5	19/2.5	12.5	10.897	4.129	0.3085

Table 4.2 discusses the parameters of the feeder line. All the conductors used are AAC type but with different diameters. Figure 4.3 presents the model of one electric pole in power distribution systems. The gap distance between the phase lines has stated clearly.

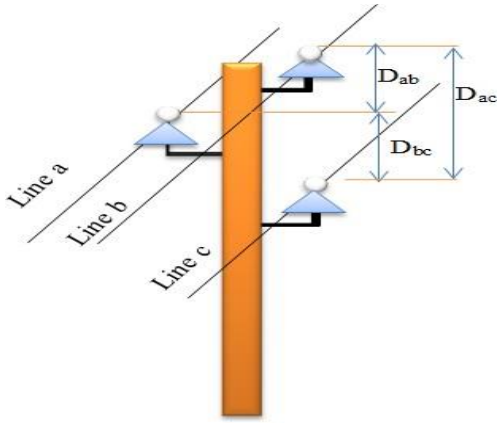

Figure 4.3: Distance between conductors

4.1.2 Fifty-nine - Bus Radial Distribution Feeder

The radial configuration of the Fifty-nine bus feeder is named as a papyrus feeder. It consists of a total number of Fifty-nine–bus feeders, of which bus-1 is taken as a reference node or slack bus, the other 47 nodes are connected to loads through step-down distribution transformer, and the remaining 12 nodes are common coupling nodes. The single line diagram of the papyrus feeder is shown in Figure 4.2. The feeder is a stranded conductor of type AAC-25, type AAC-50 and AAC-95 with a total length of 41.771 km. These overheads are used to distribute medium voltage (15 kV) power from Bahir Dar Substation-II to the distribution transformers. The conductor arrangements on the concrete pole of the distribution network are shown in Figure 4.3.

The line and load data of papyrus feeder are shown in Table 4.3.

Table 4.3: Load and line data of papyrus feeder

Sending node	Receiving node	Conductor type	Length (km)	Resistance (Ω)	Reactance (Ω)	Pload receiving (kw)	Qload receiving (KVAr)
1	2	AAC95	1.516	0.46	0.49	198	129.5
1	3	AAC95	0.791	0.24	0.25	175.2	124
3	4	AAC95	1.379	0.42	0.44	125	99
3	5	AAC95	0.458	0.14	0.13	105	79
5	6	AAC25	0.465	0.54	0.17	90.5	68
5	7	AAC25	0.563	0.66	0.21	118.69	88
5	8	AAC95	0.518	0.15	0.16	130.56	94
8	9	AAC95	0.33	0.10	0.11	0	0
9	10	AAC95	0.517	0.15	0.16	50	38
9	11	AAC95	0.379	0.11	0.12	80	57
8	12	AAC95	0.339	0.13	0.10	87	52
12	13	AAC95	0.246	0.07	0.08	0	0
13	14	AAC50	1.828	1.05	0.63	100	75
13	15	AAC50	0.645	0.37	0.22	86	50
12	16	AAC50	0.699	0.40	0.24	81	45
16	17	AAC95	1.879	0.57	0.60	90	54
16	18	AAC95	0.699	0.21	0.22	78.6	46
18	19	AAC95	0.761	0.23	0.24	49	28
18	20	AAC95	0.769	0.23	0.24	70	45
20	21	AAC25	0.592	0.69	0.22	90	58
20	22	AAC50	0.314	0.18	0.10	30	21.08
22	23	AAC50	0.48	0.27	0.16	15	6.5
22	24	AAC25	0.397	0.46	0.14	70.8	50
24	25	AAC50	0.498	0.28	0.17	0	0
24	26	AAC95	0.753	0.23	0.24	0	0
26	27	AAC50	0.482	0.27	0.16	70	50.5
26	28	AAC95	1.059	0.32	0.34	80	55.05
28	29	AAC50	2.591	1.49	0.89	85.5	53.5
28	30	AAC95	0.271	0.08	0.09	0	0
30	31	AAC25	2.047	2.41	0.76	68	38
31	32	AAC95	0.891	0.27	0.28	75	35.5
32	33	AAC50	1.398	0.80	0.40	80	48.5
32	34	AAC25	1.469	1.73	0.54	70	26.3
34	35	AAC25	0.54	0.63	0.20	40.5	16.5
34	36	AAC25	1.269	1.49	0.20	60	35.5
30	37	AAC95	0.453	0.13	0.14	90	45.8
37	38	AAC25	0.43	0.50	0.16	70	38.09
38	39	AAC25	0.512	0.60	0.19	75	39
38	40	AAC25	0.427	0.50	0.15	83	55.6
40	41	AAC25	0.649	0.76	0.24	68	44.5
40	42	AAC50	0.389	0.22	0.13	67	48.5
37	43	AAC95	0.67	0.20	0.21	0	0
43	44	AAC25	1.45	1.71	0.54	58	39.40

44	45	AAC50	0.413	0.23	0.14	82	49
44	46	AAC25	0.914	1.07	0.34	90.35	58.5
43	47	AAC50	0.401	0.23	0.13	85	47.04
47	48	AAC50	0.442	0.25	0.15	0	0
47	49	AAC50	0.447	0.25	0.15	83	45.8
49	50	AAC50	0.391	0.22	0.13	0	0
49	51	AAC50	0.462	0.26	0.16	74	38.3
51	52	AAC50	0.307	0.17	0.10	96	55.2
51	53	AAC95	0.443	0.13	0.14	0	0
53	54	AAC95	0.345	0.10	0.11	84.08	49
53	55	AAC95	0.126	0.03	0.04	0	0
55	56	AAC95	1.054	0.32	0.34	90	59
55	57	AAC50	0.391	0.22	0.13	0	0
57	58	AAC50	0.42	0.24	0.14	96	58
57	59	AAC50	0.403	0.23	0.13	109	88

4.2 Problem formulation

4.2.1 Objective Function

The main goal of the proposed study is to determine the best locations and sizes for D-STATCOMs by minimizing fitness function. It is clear that the different parts of the objective function do not have the same importance. So, each part has considered with a weight. The objective of D-STATCOM placement in the radial distribution system is to minimize the total power losses, enhancement of voltage profile and voltage stability index while satisfying the equality and inequality constraints.

Loss reduction

The total line losses in the distribution system can be calculated as follows:

$$F_1 = \sum_{i=1}^{NBr} R_i \times I_i^2 \qquad (4.7)$$

Where F_1 is the first term of objective function associated with the system losses, I_i is the current of line i, R_i is the resistance of i^{th} line, and NBr is the number of system branches.

Voltage Profile improvement

The objective function for improving the voltage profile is

$$F_2 = \sum_{i=1}^{NBus} (V - V_i)^2 \qquad (4.8)$$

Where F_2 is the second term of objective function, V_i is the bus voltage, and V is the reference voltage which is 1 p.u.

Voltage Stability Improvement

There are many indices used to check the power system security level[48]. In this section, a new steady state voltage stability index is used in order to identify the node, which has more chance to voltage collapse. The voltage stability index at each node is calculated using Equation 4.9. The node which has the low value of VSI is the weakest node and the voltage collapse phenomenon will start from that node[49]. VSI is calculated from the load flow for all the buses of the given system and the values are arranged in ascending order. The VSIs choose the sequence in which the buses are to be considered for D-STATCOM allocation, Therefore to avoid the possibilities of voltage collapse, the VSI of nodes should be maximized[50].

$$VSI(t+1) = |V_t|^4 - 4\left[P_{t+1,eff} \times X_t - Q_{t+1,eff} \times R_t\right]^2 - 4\left[P_{t+1,eff} \times R_t + Q_{t+1} \times X_t\right]|V_t|^2 \quad (4.9)$$

$$F_3 = \min(VSI(t+1)) \quad (4.10)$$

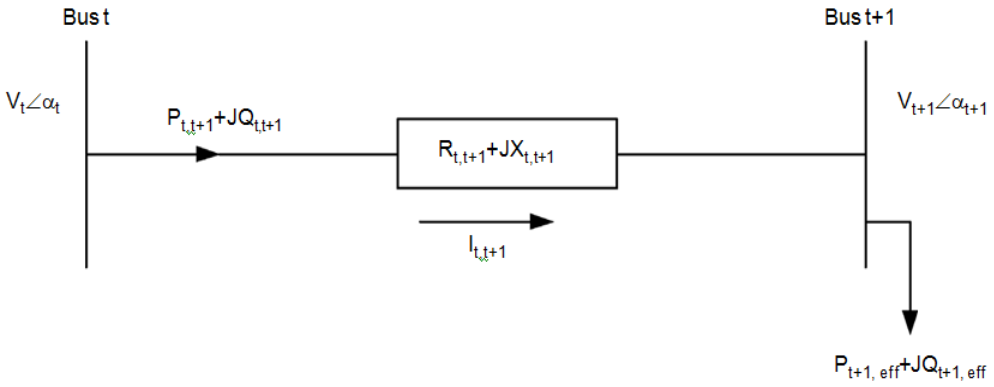

Figure 4.4: Two-bus system for VSI analysis

Where F_3 is the objective function for voltage stability index, *VSI (t+1)* is the voltage stability index at bus t+1, *t* and *t+1* are the sending and receiving bus number, $P_{t+1,\,eff}$ *and* $Q_{t+1,\,eff}$ are active and reactive power demands at bus *t+1*, respectively, V_t is the voltage of the sending bus, $R_{t,\,t+1}$, $X_{t,\,t+1}$ are the resistance and reactance of branch *t.*

The mathematical formulation of the objective function (F) is given by

$$Minimize(F) = \min(W_1 \times F_1 + W_2 \times F_2 + W_3 \times \frac{1}{F_3}) \quad (4.11)$$

$$\text{Where} \quad \sum_{n=1}^{3} W_n = 1$$

4.2.2 Choice of weighting values

The sharing of the different weights in a certain multi-objective function differs based on the engineer‘s interest. In this research work, more emphasizes is given to real power loss reduction since this results in a considerable decrease in the total cost of operation. Though, this is not to mean that the other two factors are not important. Thus taking this into consideration a study of the effect of the weights on the fitness was done so as to determine the best weights combination to adopt in coming up with the multi-objective function. During this study the values of the weights were assumed positive and restricted as follows[51]:

- W_1 was restricted between 0.5 and 0.8
- W_2 and W_3were restricted between 0.1 and 0.4

This was done so as to ensure that much emphasizes is given to the real power loss reduction index as earlier stated while at the same time ensuring that all the three indices are taken into consideration while formulating the multi-objective function.

It is also important to note that the condition $W_1+W_2+W_3=1$ has to be satisfied in each case. Table 4.4 gives the results obtained in this study.

Table 4.4: Effects of Weights on Fitness

W1	W2	W3	best fitness
0.5	0.4	0.1	0.5165
0.5	0.2	0.3	0.4010
0.5	0.25	0.25	0.3432
0.5	0.3	0.2	0.2855
0.5	0.4	0.1	0.1700
0.6	0.1	0.3	0.3903
0.6	0.2	0.2	0.2748
0.6	0.3	0.1	0.1593
0.7	0.1	0.2	0.2642
0.7	0.2	0.1	0.1487
0.8	**0.1**	**0.1**	**0.1381**

From the results presented in the above Table 4.4 the combination of weights chosen is the one which gave the minimum best fitness. Thus the weights chosen were W_1=0.8 for power loss reduction, W_2=0.1 for voltage profile improvement, and W_3=0.1 for voltage stability index and the MOF was given by;

$$F = 0.8\times F_1 + 0.1\times F_2 + 0.1\times \frac{1}{F_3} \qquad (4.\ 12)$$

4.2.3 System constraints

Voltage deviation limit

The system voltage in all buses should be in an acceptable range

$$V_m^{\min} \le |V_m| \le V_m^{\max} \quad (4.13)$$

The system voltage is constrained with $0.95\text{pu} \le V_m \le 1.05$ pu

Reactive power compensation

The reactive power injected by D-STATCOM to the system is limited by a lower and upper bound as given in following

$$Q_m^{\min} \le |Q_m| \le Q_m^{\max} \quad (4.14)$$

The reactive power injected by D-STATCOM is limited by $100\text{KVar} \le Q_m \le 1250\text{KVAr}$

Thermal limit

The power flow through the lines is limited by the thermal capacity of lines:

$$|S_{ij} \le S_{ij\max}| \quad (4.15)$$

The power flow through the lines is limited with $S_{ijmax}=100\text{MVA}$

4.3 Steps for the optimization algorithm

The proposed optimization algorithm is implemented for finding an optimal D-STATCOM placement and sizing in papyrus radial distribution feeder (RDS) using the following steps:

1. Select the number of D-STATCOM units to be installed.
2. Read line and load data of radial distribution system
3. Set the lower and upper bounds of system constraints, particle swarm optimization algorithm control parameters (Population size, Wmax, Win, C_1, and C_2) and Maximum iteration.
4. Generate an initial random particle infeasible area. Each particle indicates an optimal size and sits for D-STATCOM.
5. Run the base case load flow algorithm and compute voltage profile at each bus, the real and reactive power loss of lines.
6. Developing bus based voltage stability index method for selecting candidate buses for placement of D-STATCOM.

7. Apply all steps for particle swarm optimization algorithm and optimized the fitness function from Fig.3.12.
8. Select an optimal solution(Optimal sizing and placement)
9. Run the direct load flow algorithm for network with D-STATCOMs integration and compute voltage profile at each bus, the real and reactive power loss of lines.
10. Display an optimal solutions

CHAPTER FIVE

5. RESULTS AND DISCUSSION

In this chapter, the results obtained using load flow, PSO and VSI methods have been presented. The algorithm outlined in the previous chapter is implemented and programmed in Mat lab 2015a. The main codes programmed according to the implementation steps of the proposed algorithm that have been given in Appendix-B. Parameters for PSO algorithm implementation is shown below in Table 5.1.

Table 5.1: Parameter value for PSO simulation

Population size	30	C_2	2
No of iteration	30	W_{max}	0.9
C_1	2	W_{min}	0.4

Based on the collected data that are given in Table 4.3 backward forward sweep load flow algorithm was run and from this, the initial power loss, bus voltage, and voltage stability index of the feeder was obtained. To obtain the optimal placement and size of the D-STATCOM, a bus-based voltage stability index analysis guided the PSO algorithm was simulated. The simulation results for proposed system are tested into six cases:

Case 1: System without D-STATCOM

Case 2: System with single D-STATCOM

Case 3: System with two fixed size D-STATCOM

Case 4: System with two variable sizes D-STATCOM

Case 5: System with three fixed size D-STATCOM

Case 6: System with three variable sizes D-STATCOM

5.1 Case 1: System without D-STATCOM

In Table 5.2 shows that the base case real and reactive power losses, voltage profile, and voltage stability index of papyrus feeder. The real and reactive power losses of the feeder are 131.7142 kW and 111.3471 KVAr. The minimum voltage magnitude of 0.9434 p.u and minimum VSI of the system is 0.7920 p.u without installing the D-STATCOM. The base case voltage profile and stability index is shown in Figure 5.1 & 5.2 respectively.

Table 5.2: base case papyrus feeder performance

NO	Parameters	Base case(Case 1)

1	Active power loss	131.7142 KW
2	Reactive power loss	111.3471 KVAr
3	Minimum VSI	0.7920@ bus 36
4	Minimum voltage	0.9434@ bus 36

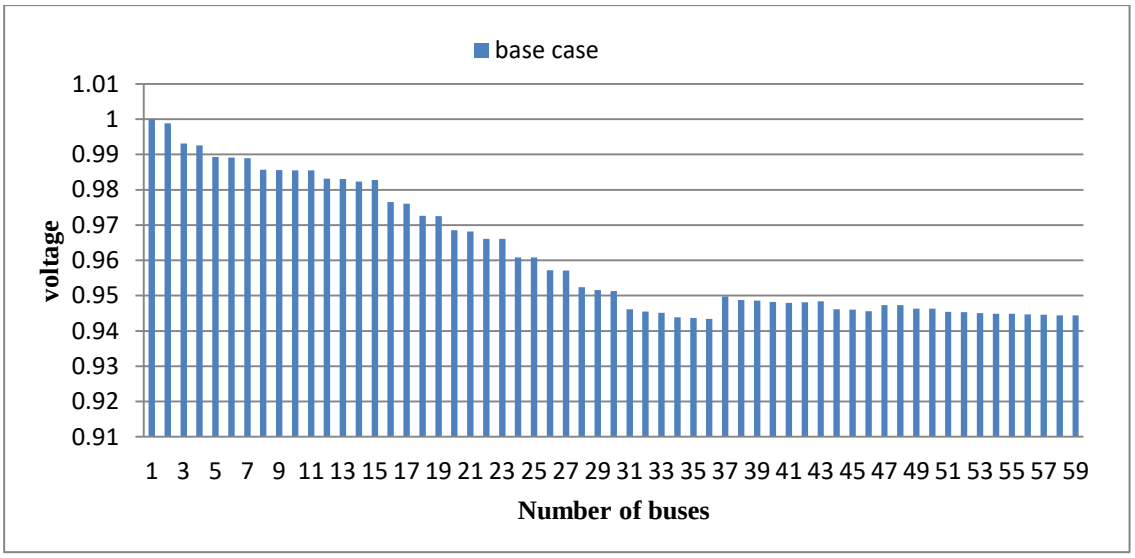

Figure 5.1: Base case voltage profile of papyrus feeder

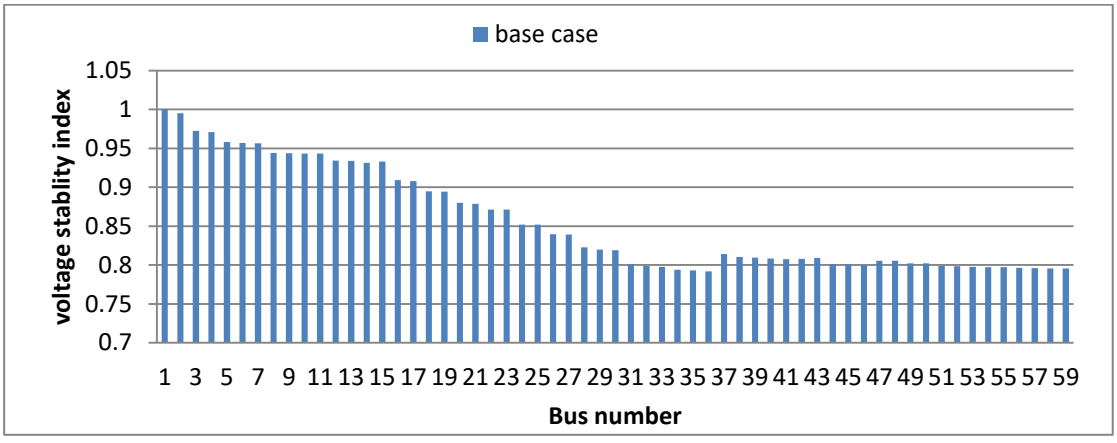

Figure 5.2: Base case voltage stability index of papyrus feeder

Table 5.3: Base case power flow analysis

Bus No.	Voltage magnitude(p.u)	Bus No.	Voltage magnitude(p.u)	Bus No	Voltage magnitude(p.u)
1	1.0000	21	0.9682	41	0.9479
2	0.9988	22	0.9661	42	0.9481
3	0.9931	23	0.9661	43	0.9484
4	0.9926	24	0.9608	44	0.9461
5	0.9893	25	0.9608	45	0.9460
6	0.9891	26	0.9572	46	0.9456
7	0.9889	27	0.9571	47	0.9473
8	0.9857	28	0.9524	48	0.9473
9	0.9856	29	0.9516	49	0.9463
10	0.9855	30	0.9513	50	0.9463
11	0.9855	31	0.9461	51	0.9454
12	0.9831	32	0.9455	52	0.9453
13	0.9830	33	0.9451	53	0.9450
14	0.9823	34	0.9439	54	0.9449
15	0.9828	35	0.9437	55	0.9449
16	0.9765	36	0.9434	56	0.9447
17	0.9761	37	0.9498	57	0.9446
18	0.9726	38	0.9488	58	0.9444
19	0.9725	39	0.9486	59	0.9444
20	0.9685	40	0.9482		

Table 5.4: Base case voltage stability index of each bus

Bus No.	VSI (p.u)	Bus No.	VSI (p.u)	Bus No.	VSI (p.u)	Bus No.	VSI (p.u)
1	1.0000	18	0.8948	35	0.7932	52	0.7984
2	0.9952	19	0.8945	36	0.7920	53	0.7974
3	0.9726	20	0.8800	37	0.8139	54	0.7972
4	0.9709	21	0.8787	38	0.8105	55	0.7971
5	0.9580	22	0.8712	39	0.8096	56	0.7963
6	0.9596	23	0.8711	40	0.8084	57	0.7961
7	0.9563	24	0.8521	41	0.8074	58	0.7956
8	0.9440	25	0.8521	42	0.8080	59	0.7955
9	0.9436	26	0.8395	43	0.8089		
10	0.9434	27	0.8390	44	0.8014		
11	0.9433	28	0.8227	45	0.8009		
12	0.9342	29	0.8199	46	0.7995		
13	0.9338	30	0.8188	47	0.8053		
14	0.9312	31	0.8012	48	0.8053		
15	0.9331	32	0.7990	49	0.8019		
16	0.9093	33	0.7977	50	0.8019		
17	0.9079	34	0.7937	51	0.7987		

5.2 Case 2: System with single D-STATCOM

Table 5.5 shows the comparison of real and reactive power losses, voltage profile, voltage stability index, locations, optimal size (KVAr) for the proposed system. In case 2 system with single D-STATCOM integration shows a clear improvement in real and reactive power losses have been reduced to 98.7441kW (i.e. percentage of reduction is 25.0315%), 83.230kVAr (i.e. percentage of reduction is 25.2517%), minimum voltage with compensating device improves to 0.9567 p.u, and minimum VSI increases to 0.8377 p.u after installing the D-STATCOM. The optimal size of D-STACOM is 1250 KVAr and sits in bus 37 of the radial distribution network.

Table 5.5: performance evaluation of case 2

NO	Parameters	Base case	PSO(Case 2)
1	Active power loss	131.7142 KW	98.7441KW
2	Reactive power loss	111.3471 kVAr	83.2300 KVAr
3	Minimum VSI	0.7920 p.u	0.8377 p.u
4	Minimum voltage	0.9434 p.u	0.9567 p.u
5	D-STATCOM location	----------	37
6	D-STATCOM Size	----------	1250 kVAr
7	Active power loss %	----------	25.0315%
8	Reactive power loss %	----------	25.2517%

From Figure 5.3 & 5.4 below, it is clearly shown that the voltage profile and stability index of the operated network before and after compensation with single D-STATCOM. The feeder becomes more stable after compensation.

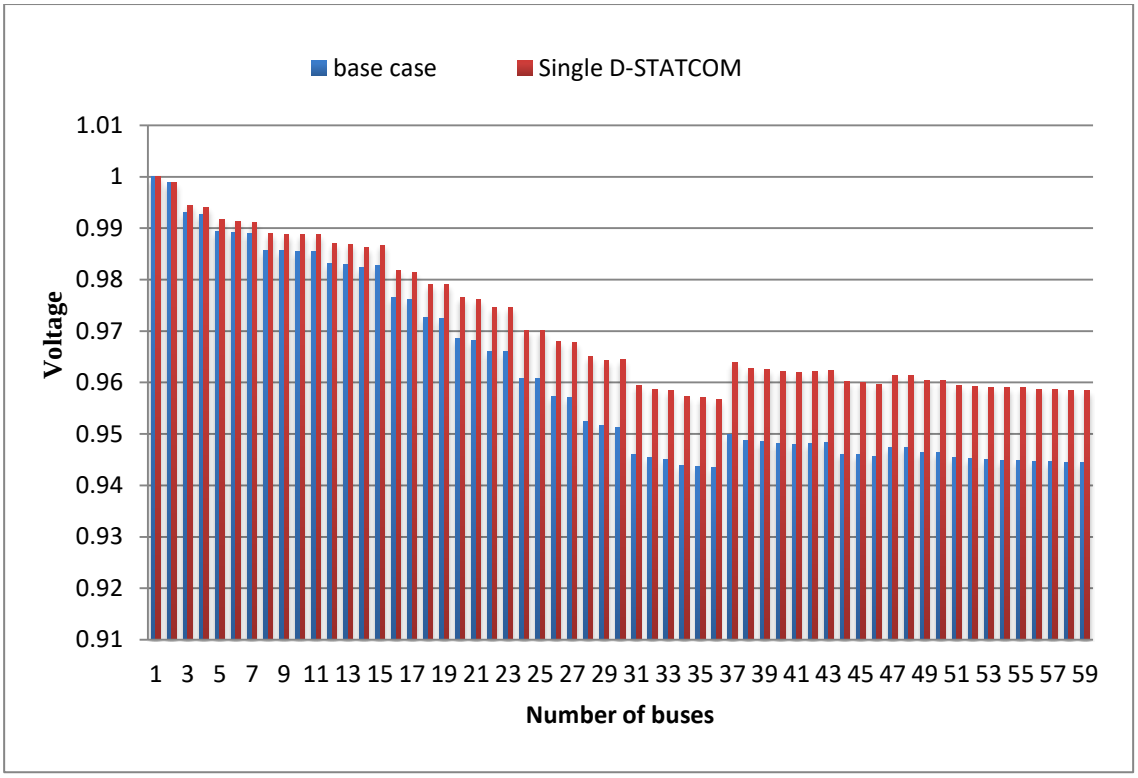

Figure 5.3: voltage profile for case 2

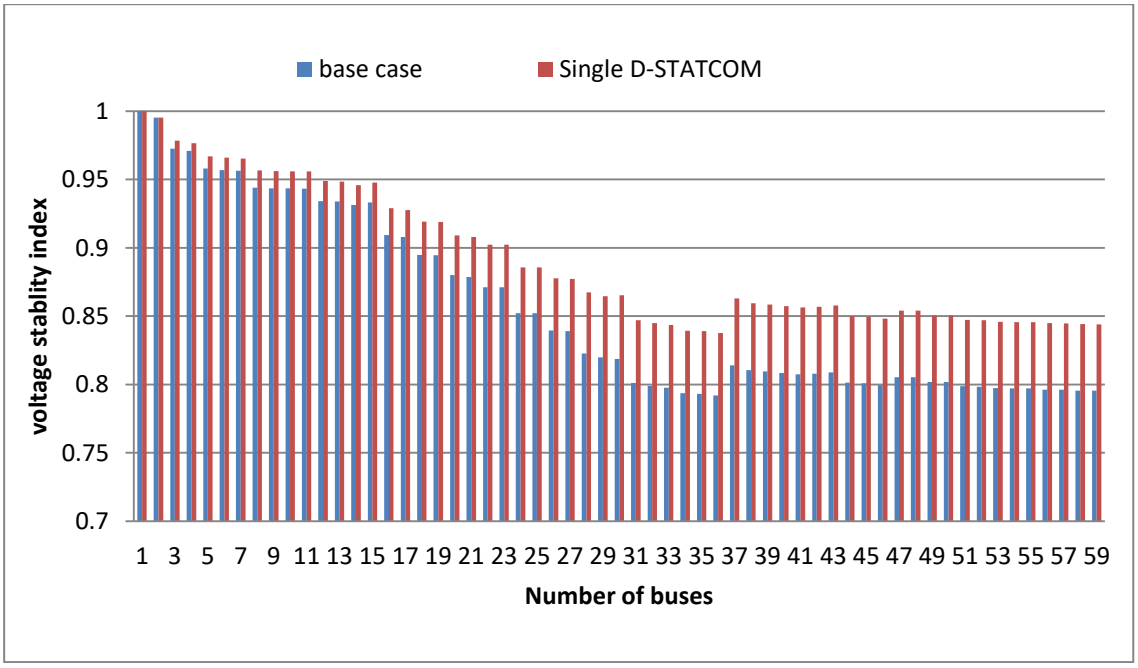

Figure 5.4: voltage stability index for case 2

5.3 Case 3: System with two fixed size D-STATCOMs

Table 5.6 shows the comparison of real and reactive power losses, voltage profile, Voltage stability index, locations, optimal size (KVAr) for the proposed method. In case 3 system with two fixed size of D-STATCOM shows a clear improvement in the real and reactive power losses have been reduced to 97.9193kW (i.e. percentage of reduction is 25.6577%), 82.5436kVAr (i.e. percentage of reduction is 25.8682%), minimum voltage with compensating device improves to 0.9567 p.u, and minimum VSI increases to 0.8378 p.u after installing the D-STATCOM. The optimal size of D-STACOM is two 625KVAr and sits in the bus 50 and 30 of radial distribution network.

Table 5.6: Performance evaluation of case 3

NO	Parameters	Base case	PSO(Case 3)
1	Active power loss	131.7142 KW	97.9193 KW
2	Reactive power loss	111.3471 kVAr	82.5436 KVAr
3	Minimum VSI	0.7920 p.u	0.8378 p.u
4	Minimum voltage	0.9434 p.u	0.9567 p.u
5	D-STATCOM location	----------	50 30
6	D-STATCOM Size	----------	625 KVAr 625 KVAr
7	Active power loss %	----------	25.6577%
8	Reactive power loss %	----------	25.8682%

From Figure 5.5 & 5.6 below, it is clearly shown that the voltage profile and stability index of the operated network before and after compensation with two fixed D-STATCOMs. The feeder becomes more stable after compensation.

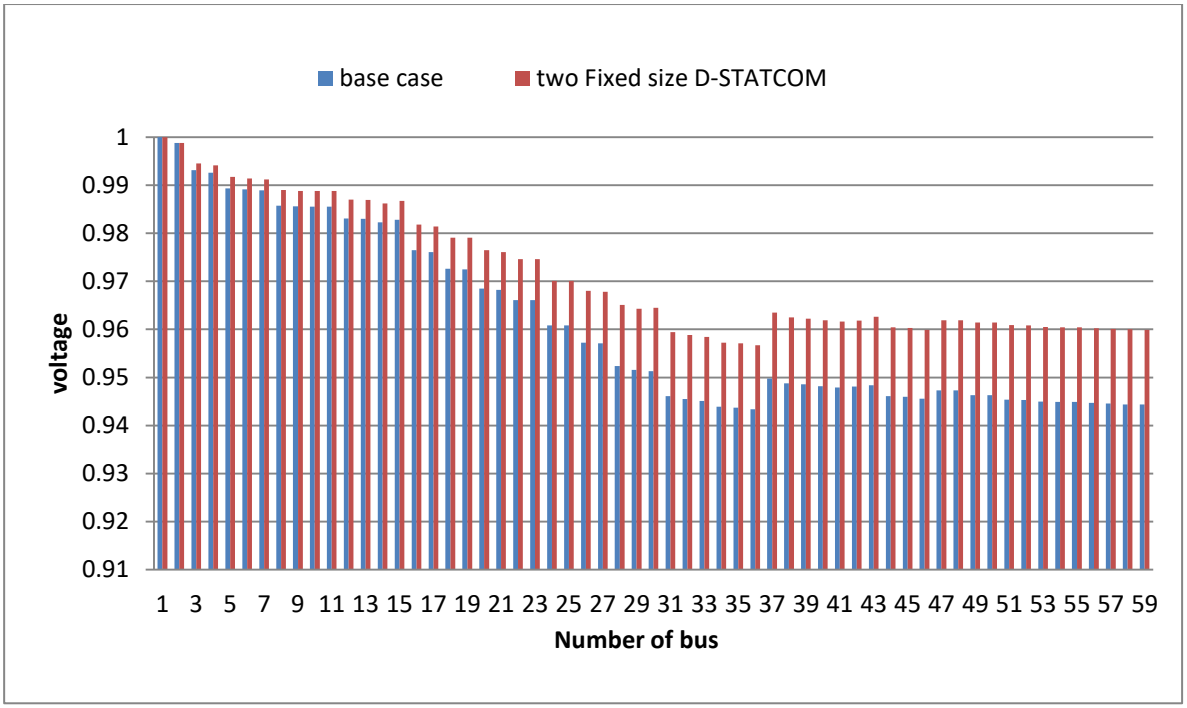

Figure 5.5: Voltage profile for case 3

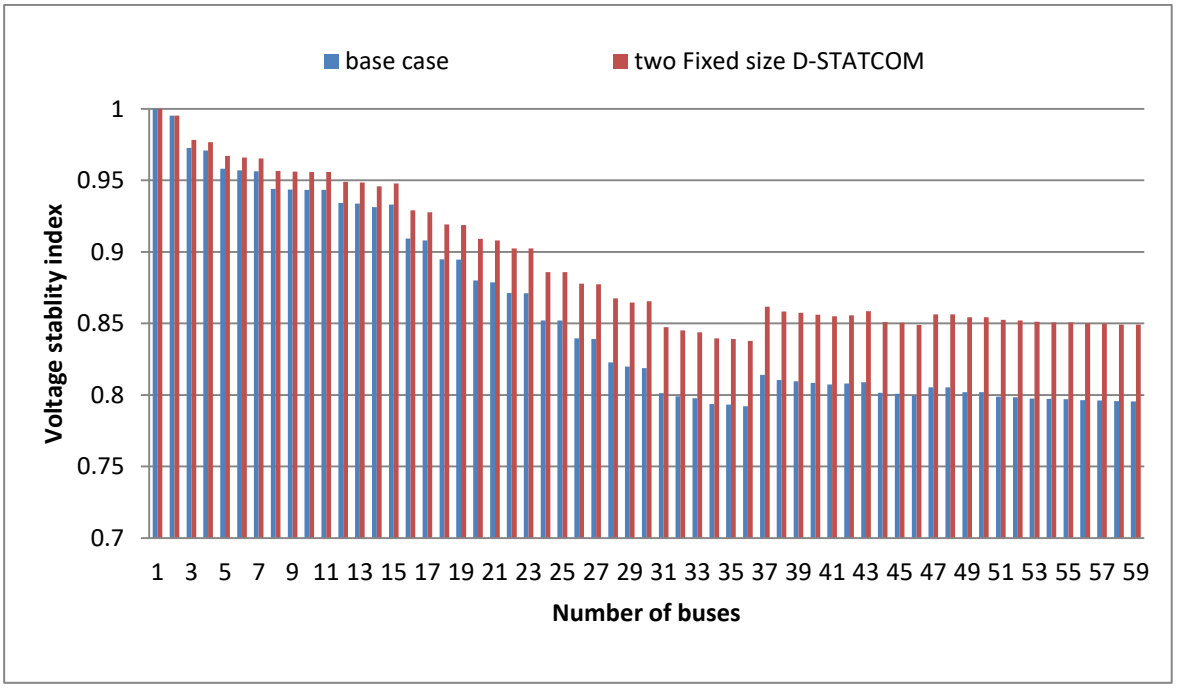

Figure 5.6: Voltage stability index for case 3

5.4 Case 4: System with two variable size D-STATCOMs

Table 5.7 shows the comparison of real and reactive power losses, voltage profile, voltage stability index, locations, optimal size (KVAr) for the proposed method. In case 4 system with two variable size of D-STATCOM shows a clear improvement in the real and reactive power losses have been reduced to 95.9891kW (i.e. percentage of reduction is 27.1232%), 80.5628kVAr (i.e. percentage of reduction is 27.6472%), minimum voltage with compensating device improves to 0.9597 p.u, and minimum VSI increases to 0.8481 p.u after installing the DSTATCOM. The optimal sizes of D-STACOMs are 578 and 1250 KVAr and sit in buses 18 and 37 respectively.

Table 5.7: Performance evaluation of case 4

NO	Parameters	Base case	PSO(Case 4)
1	Active power loss	131.7142 KW	95.9891 KW
2	Reactive power loss	111.3471 kVAr	80.5628KVAr
3	Minimum VSI	0.7920 p.u	0.8481 p.u
4	Minimum voltage	0.9434 p.u	0.9597 p.u
5	D-STATCOM location	----------	18 37
6	D-STATCOM Size	----------	578 KVAr 1250 KVAr
7	Active power loss %	----------	27.1232%
8	Reactive power loss %	----------	27.6472%

From Figure 5.7 & 5.8 below, it is clearly shown that the voltage profile and stability index of the operated network before and after compensation with two variable size of D-STATCOM .The feeder becomes more stable after compensation.

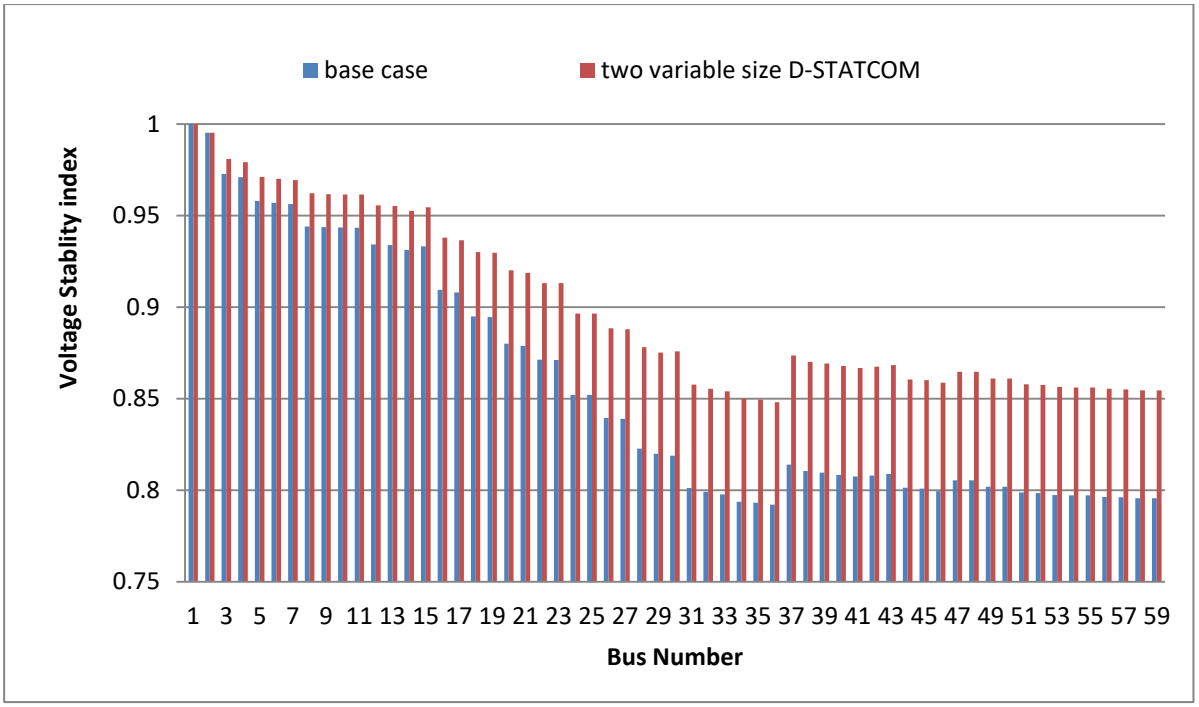

Figure 5.7: voltage stability index for case 4

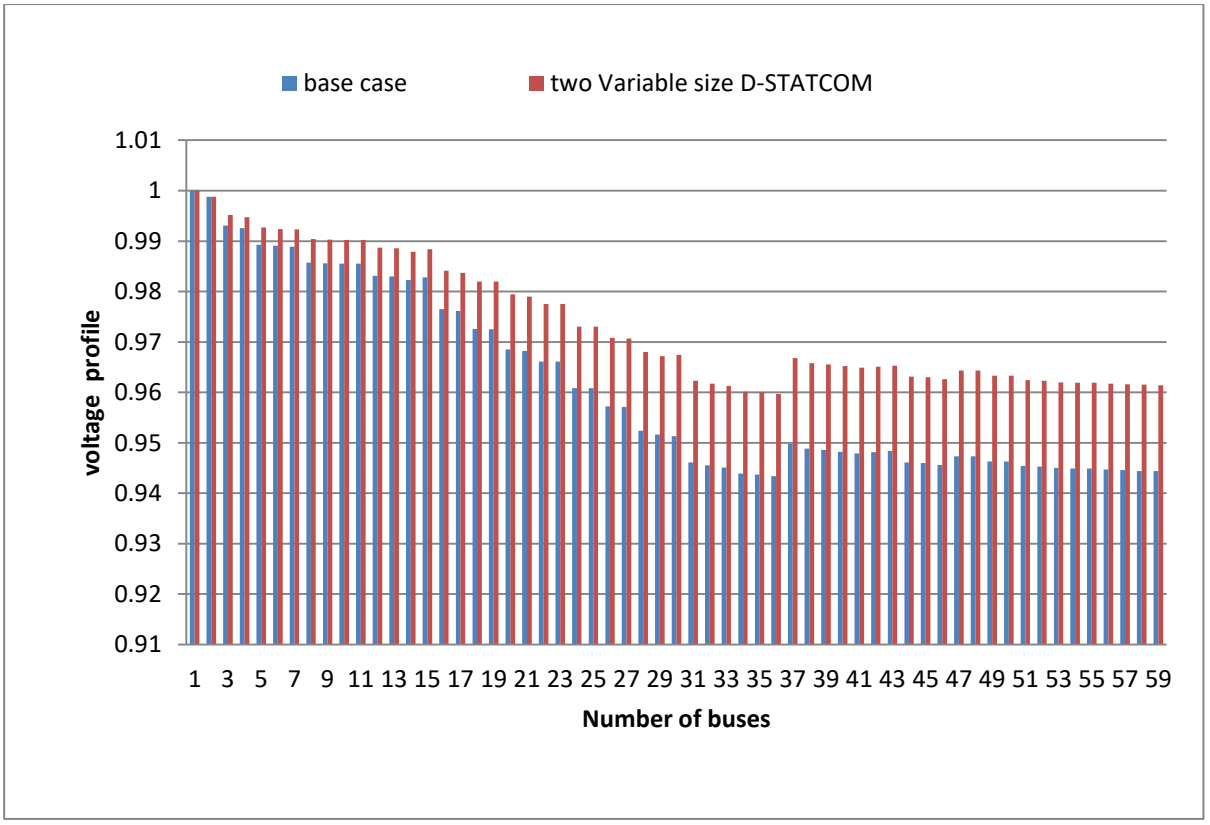

Figure 5.8: voltage profile for case 4

5.5 Comparison of two D-STATCOM placement integration

Figure 5.9 & 5.10 shown that a comparative analysis of voltage profile and voltage stability index of papyrus feeder for placement of two D-STATCOM with equal fixed and variable size respectively. A clear improvement in system performance is shown for the installation of two variable sizes D-STATCOM over fixed size D-STATCOMs.

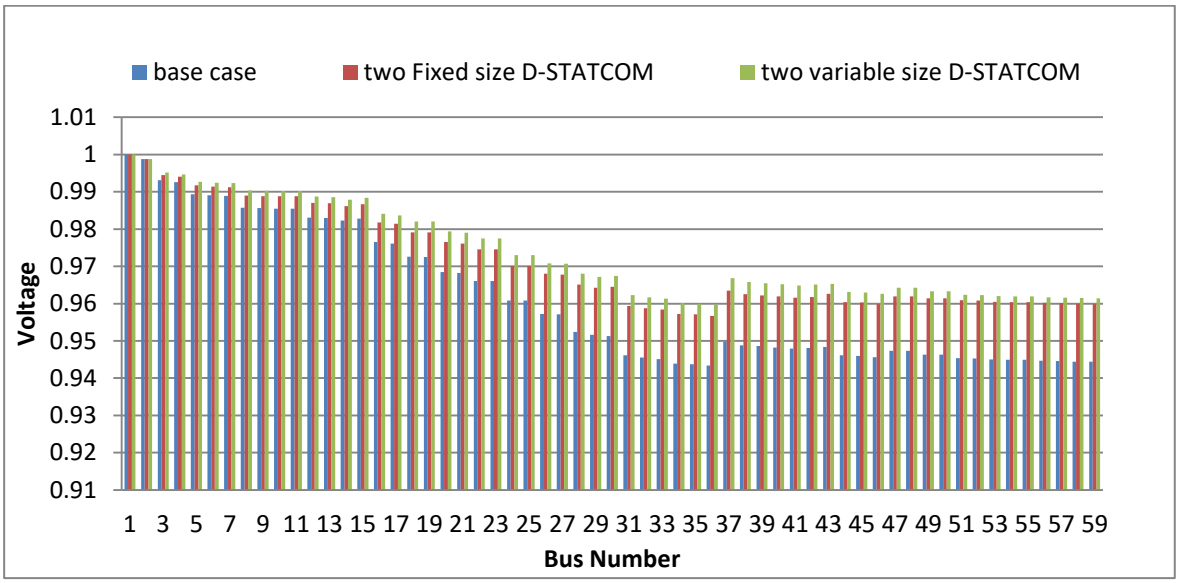

Figure 5.9: Comparative analysis of the voltage profile for case 3 and 4

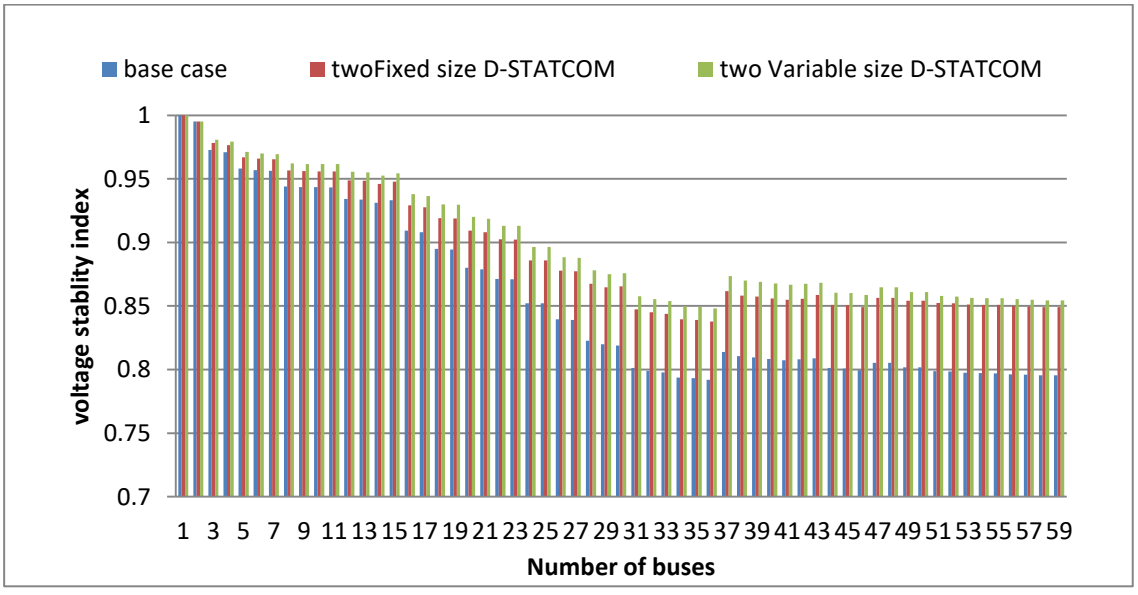

Figure 5.10: Comparative analysis of voltage stability index for case 3 and 4

5.6 Case 5: System with three fixed size D-STATCOMs

Table 5.8 shows the comparison of real and reactive power losses, voltage profile, voltage stability index, locations, optimal size (KVAr) for the proposed method. In case 5 system with three fixed size D-STATCOM shows a clear improvement in the real and reactive power losses have been reduced to 97.7121kW (i.e. percentage of reduction is 25.8150 %), 82.4142kVAr (i.e. percentage of reduction is 25.9844 %), minimum voltage with compensating device improves to 0.9567 p.u, and minimum VSI increases to 0.8373 p.u after installing the D-STATCOMs. The optimal sizes of D-STACOM are three 417KVAr and sit in bus 28, 43, and 53 respectively.

Table 5.8: Performance evaluation of case 5

NO	Parameters	Base case	PSO(Case 5)
1	Active power loss	131.7142 KW	97.7121 KW
2	Reactive power loss	111.3471 KVAr	82.4142 KVAr
3	Minimum VSI	0.7920 p.u	0.8373 p.u
4	Minimum voltage	0.9434 p.u	0.9567 p.u
5	D-STATCOM location	----------	28 43 53
6	D-STATCOM Size	----------	417 KVAr 417 KVAr 417 KVAr
7	Active power loss %	----------	25.8150 %
8	Reactive power loss %	----------	25.9844 %

From Figure 5.11 & 5.12 below, it is clearly shown that the voltage profile and stability index of the operated network before and after compensation with three fixed size D-STATCOMs. The feeder becomes more stable after compensation.

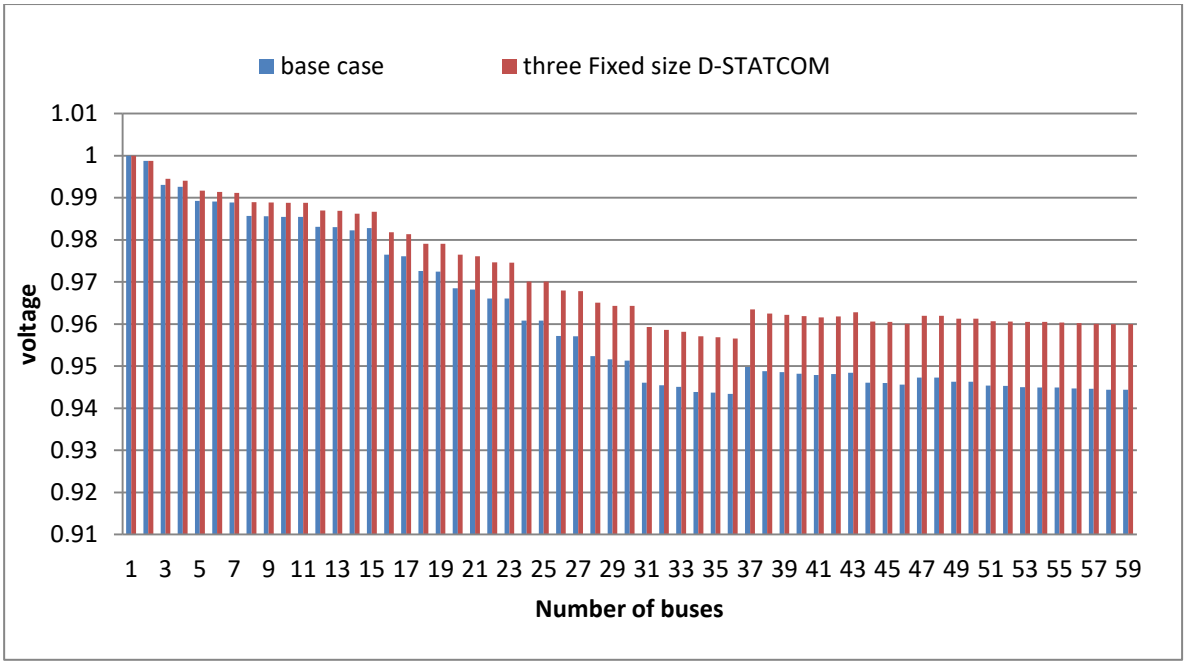

Figure 5.11: voltage profile for case 5

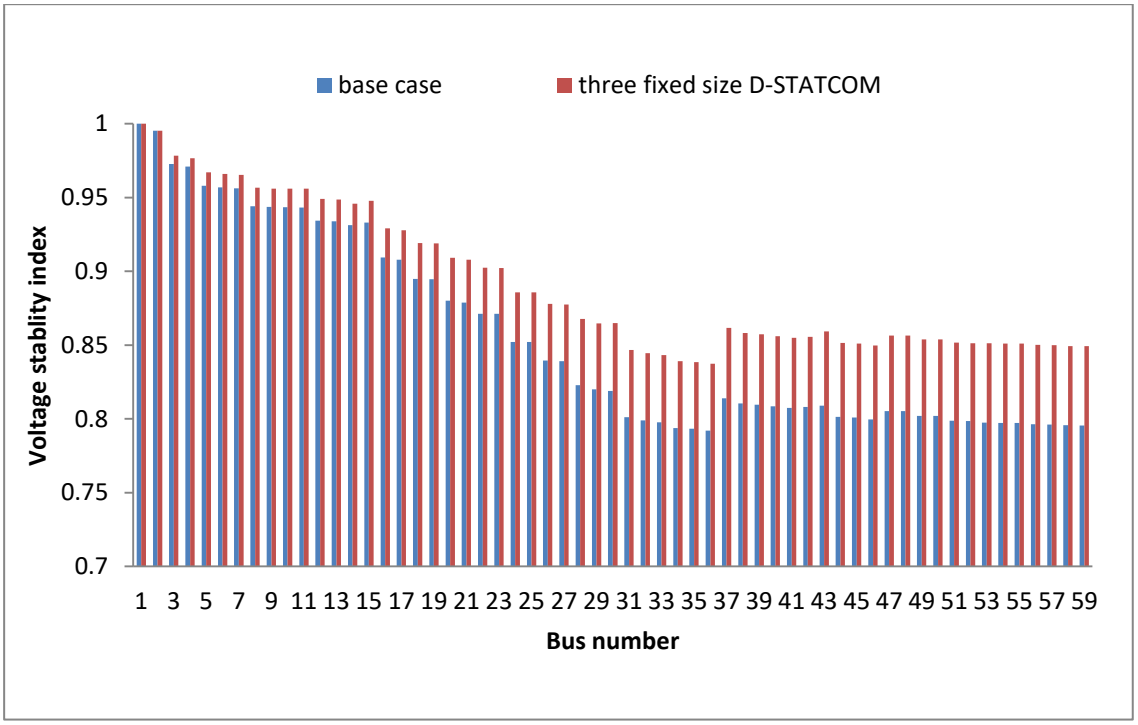

Figure 5.12: voltage stability index for case 5

5.7 Case 6: System with three variable size D-STATCOMs

Table 5.9 shows the comparison of real and reactive power losses, voltage profile, voltage stability index, locations, optimal size (KVAr) for the proposed method. In case 6 system with three variable size of D-STATCOM shows a clear improvement in, the real and reactive power losses have been reduced to 95.2542kW (i.e. percentage of reduction is 27.6812 %), 80.0047kVAr (i.e. percentage of reduction is 28.1484 %), minimum voltage with compensating device improves to 0.9612 p.u, and minimum VSI increases to 0.8534 p.u after installing the DSTATCOM. The optimal sizes of D-STACOMs are 830, 226, and 1250KVAr and sit in buses 9, 59 and, 30 respectively.

Table 5.9: Performance evaluation of case 6

NO	Parameters	Base case	PSO(Case 6)
1	Active power loss	131.7142 KW	95.2542 KW
2	Reactive power loss	111.3471 kVAr	80.0047 KVAr
3	Minimum VSI	0.7920 p.u	0.8534 p.u
4	Minimum voltage	0.9434 p.u	0.9612 p.u
5	D-STATCOM location	----------	9 59 30
6	D-STATCOM Size	----------	830 KVAr 226 KVAr 1250 KVAr
7	Active power loss %	----------	27.6812 %
8	Reactive power loss %	----------	28.1484 %

From Figure 5.13 & 5.14 below, it is clearly shown that the voltage profile and stability index of the operated network before and after compensation with three variable D-STATCOMs. The feeder becomes more stable after compensation.

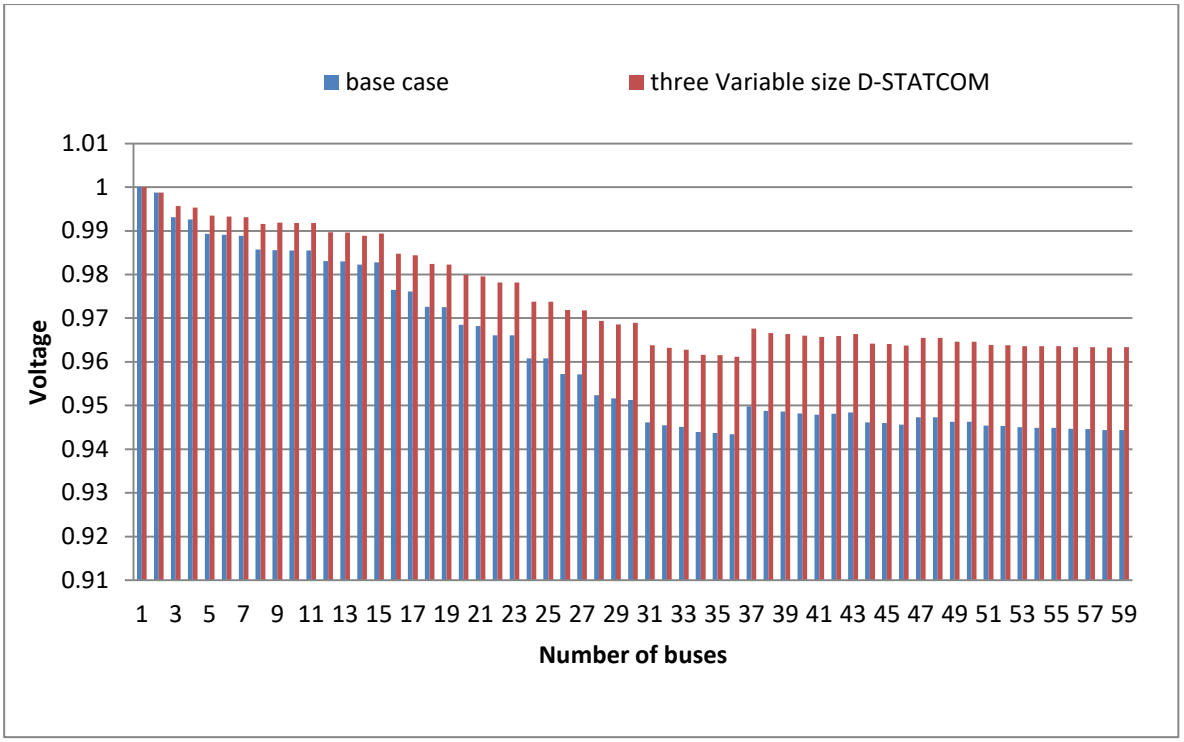

Figure 5.13: voltage profile for case 6

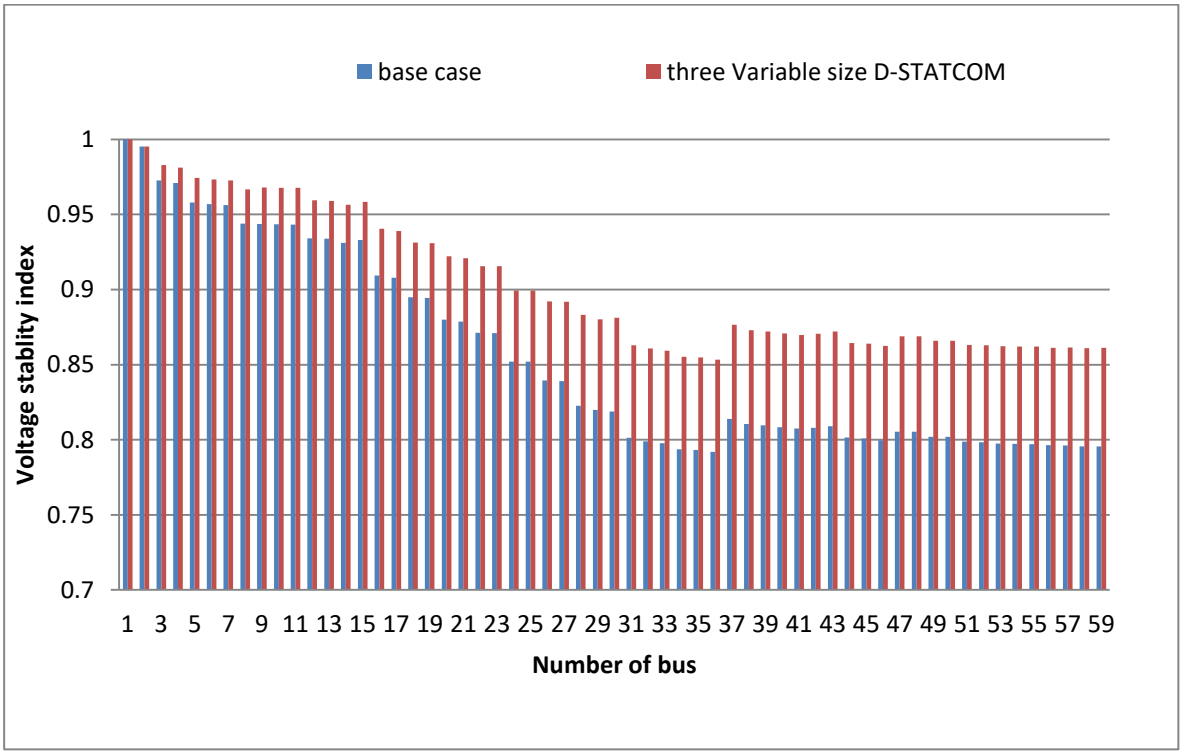

Figure 5.14: voltage stability index for case 6

5.8 Comparison of three D-STATCOM placement integration

Figure 5.15 & 5.16 shown that a comparative analysis of voltage profile and voltage stability index for placement of three D-STATCOM with equal fixed and variable size respectively. A clear improvement in system performance is shown for the installation of three variable sizes D-STATCOMs over three fixed size D-STATCOMs**.**

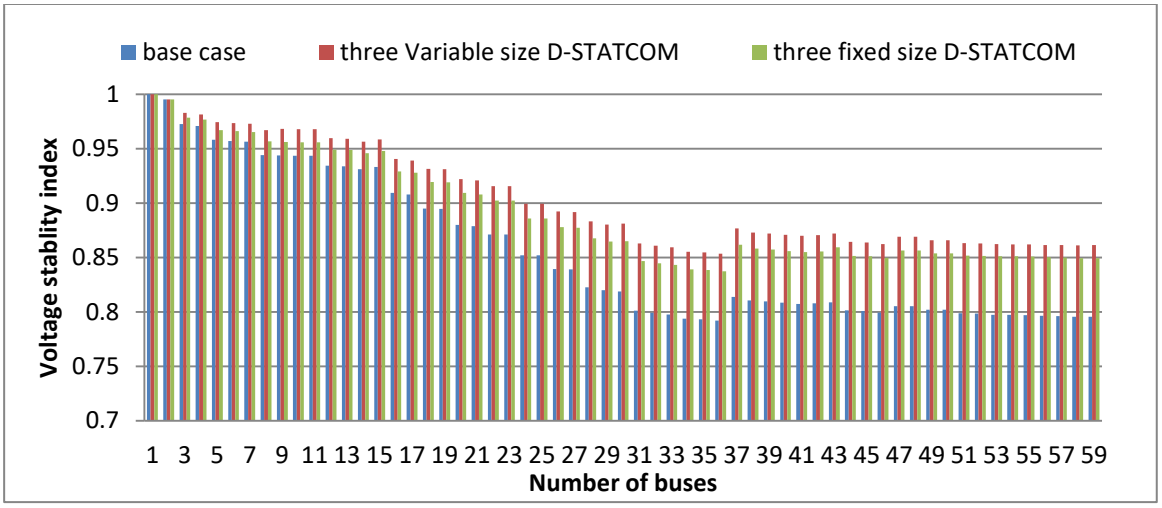

Figure 5.15: Comparative analysis of voltage stability for case 5 and 6

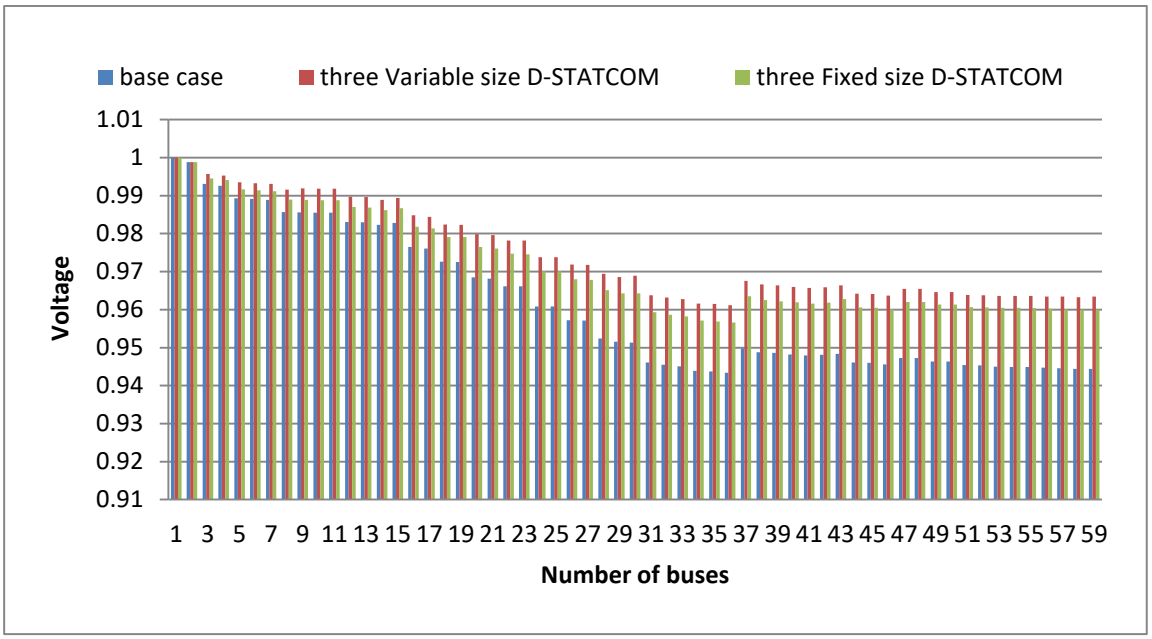

Figure 5.16: Comparative analysis of voltage profile for case 5 and 6

5.9 Comparison of all tested cases

Figure 5.17 & 5.18 shown that a comparative analysis of voltage profile and voltage stability index for placement of D-STATCOMs units for all tested cases respectively. A clear improvement in system performance is shown for the installation of three variable sizes D-STATCOM.

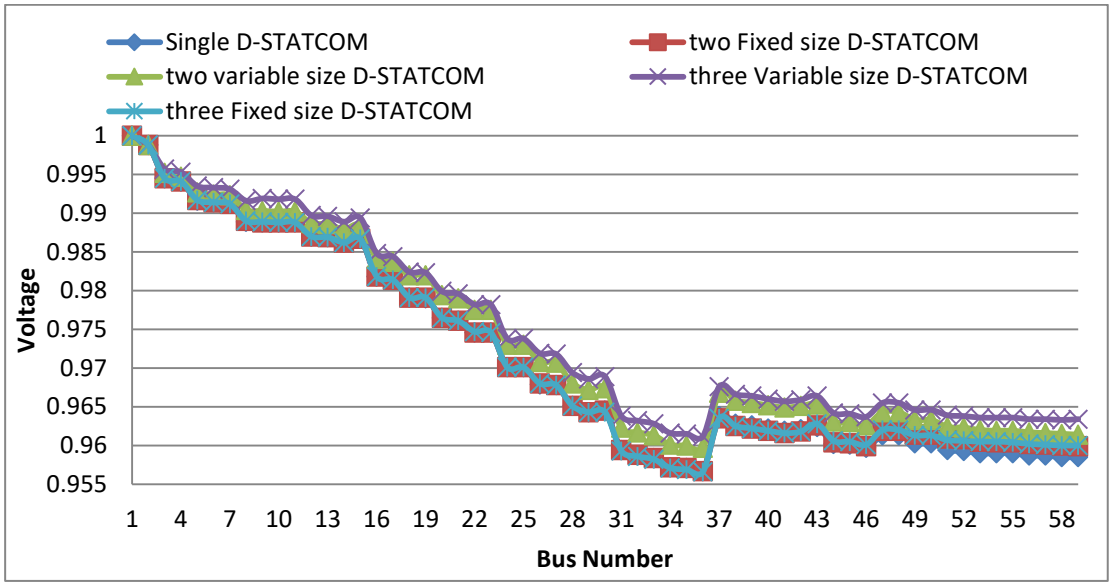

Figure 5.17: Voltage profile of papyrus feeder for all tested cases

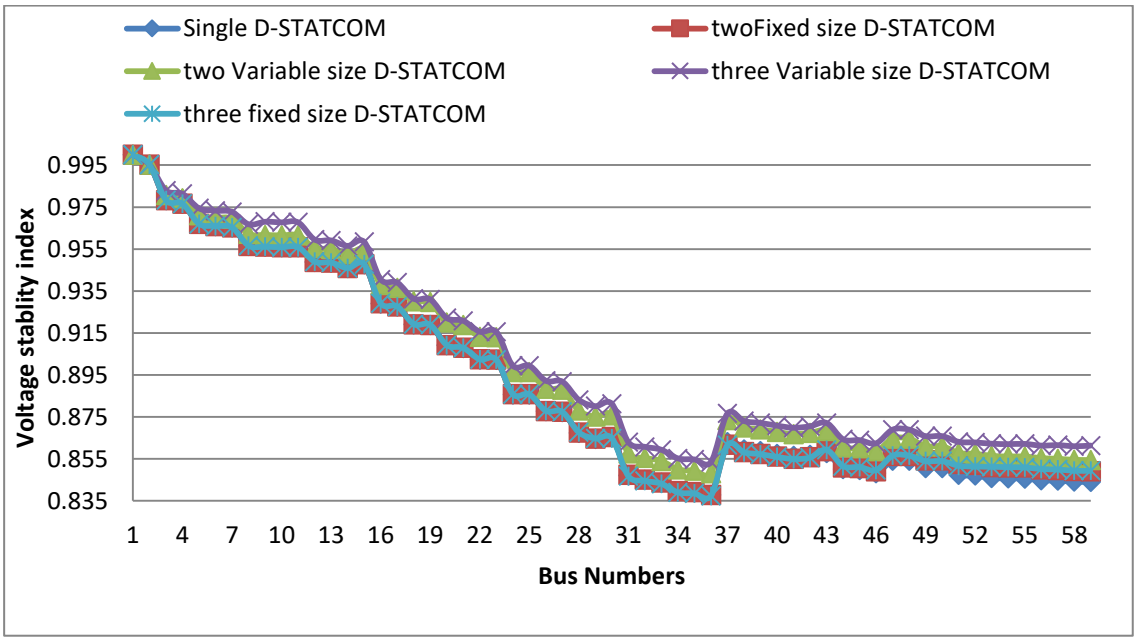

Figure 5.18: Voltage stability index of papyrus feeder for all tested cases

5.10 Economic Impact of Integrating D-STATCOM

Energy losses of Papyrus feeder before D-STATCOM installation

Annual energy loss of papyrus feeder = Ploss*8760hrs

= 131.72 KW * 8760hrs

= 1, 153,779.6 KWhrs

Ethiopian Electric Utility tariff order for Industrial low voltage/Tariff 10/ which is given in appendix E [53]. A 15KV at peak category rate/Eth Birr is 0.6943cent/KWh

Cost of energy loss = Eloss*E.C

= 1,153,779.6 KWhrs* 0.6943 birr/KWh

= 801,069 birr

The results show that before installing D-STATCOM the energy loss cost is 801,069 birr.

Energy losses of the papyrus feeders after D-STATCOM installation

Annual energy loss reduction of Papyrus feeders = $P_{loss\ reduction}$*8760hrs

= 32.9759KW * 8760hrs

= 288,868.884 KWhrs

Cost of energy loss reduction = $E_{loss\ reduction}$*E.C

= 288,868.84 KWhrs * 0.6943 birr/KWh

= 200,561.66 birr

After installation of D-STATCOM through the papyrus feeder with optimal size and placement, the annual energy loss cost is minimized from 801,069 birr to 600,507.33birr. This means it reduced almost 25.03% energy cost reduction after compensation by D-STATCOM. The Cost of D-STATCOM per KVAr is 960 birr[52]. The total cost of 1250KVAr size D-STATCOM is 1,200,000 birr.

Installation Cost of D-STATCOM [54] for

- One unit of D-STACOM below 400Kvar size is 90,000 birr
- One unit of D-STATCOM between 400KVAr-1500Kvar size is 150,000 birr
- One unit of D-STATCOM above 1500KVAr size is 240,000 birr

Now the total cost for D-STATCOM installation (Cost for equipment and installation cost) is 1, 350, 000 birr.

The payback period in a year can be calculated by using the following equation[52]:

$$Pay-back = \frac{Total\ cost}{Energy\ cost}$$

$$= \frac{1,350,000}{200,561.66} = 6.73$$

Table 5.10 Cost comparison between tested cases

No	Test cases	Cost of energy loss before	Cost energy loss With D-STATCOM	Pay-back period(years)
1	Case 1	801,069 birr	.....	.....
2	Case 2	801,069 birr	200,561.66 birr	6.73
3	Case 3	801,069 birr	205,542.88birr	7.29
4	Case 4	801,069 birr	217,282.48birr	9.45
5	Case 5	801,069 birr	206,803.09birr	7.97
6	Case 6	801,069 birr	221,752.20birr	11.74

CHAPTER SIX

6. CONCLUSION AND RECOMMENDATION

6.1 Conclusion

In conclusion, this research work showed the formulation and implementation of a PSO algorithm to help in reducing system power loss, improving voltage profile, and voltage stability index by optimizing the location and size of D-STATCOMs units. The bus-based voltage stability index was formulated and used effectively in reducing the search space for the algorithm. A direct load flow analysis method was applied to find system voltage, active and reactive power losses. A multi-objective function comprising of total active power loss, voltage profile and voltage stability index improvement was formulated for the optimization algorithm. The effectiveness and applicability of the approach have been demonstrated on Bahir Dar papyrus feeder which has a 59-bus radial distribution network for a steady-state constant load model.

The simulation results were tested by considered different cases based on the type, and number of D-STATCOMs. Single, two with fixed size, two with variable, three with fixed, and three with variable size of D-STATCOMs cases were considered. From the simulation result the percentage reduction in real power loss was 25.0315%, 25.6577%, 27.1232%,25.8152%, and 27.6812% while the percentage reactive power loss reduction was 25.0315%, 25.6577% ,27.1232%,25.8150%,and 28.1484% for case 2, case 3, case 4, case 5 and case 6 of D-STATCOM installation respectively. The voltage profile of the operated network is generally improved in the acceptable IEEE range .The voltage stability index of the operated network is also shown an improvement from the base case after D-STATCOMs integration.

After implementing the PSO method to study the effects of D-STATCOM penetration on power losses, voltage stability, and voltage profile it was clearly shown that the system power losses reduced with the introduction of multiple and three D-STATCOMs into the network .The voltage profile and stability index also behaved in a similar manner where further D-STATCOM introduced to the network system performance was increased.

The total annual cost reduction for cases 2, 3, 4, 5, and 6 are 200,561.88birr, 205,542.88 birr, 217,282.48birr, 206,803.09birr, and 221,752.20birr while the payback period is

6.73,7.29,9.45,7.97,and 11.74 years respectively. Due to the installation cost, maintenance cost, and the payback period of multiple and three D-STATCOMs is much higher than single D-STATCOMs; it is recommended to integrate single D-STATCOM of size 1250KVAr in bus 37. Moreover the overall of system performance is increased after the integration of D-STATCOMs.

Finally, this research puts an optimal size and placement of D-STATCOM units for the case study area of papyrus feeder. A single 1250KVAr size D-STATCOM unit is an optimal economical solution for the system performance improvement as compared with other tested cases. A STATCOM unit supplier of size 1250KVAr was searched for the case study area and a sinopack company gives a better price as compared with other supplier company's .A total installation and price of STATCOM unit 1,350,000.00 birr is given by the company. The product specification and photos for references in installation is given in APPENDIX F.

6.2 Recommendation

- This thesis works only conducted on the papyrus feeder line, future works should take the same methodology for the other feeder lines of the substation.
- Industries and high reactive power consumed customers should install D-STATCOM.
- Use other optimization algorithms like GA, Hybrid GA-PSO, Immune, and BFOA algorithm for optimal placement and sizing of D-STATCOM.
- The possibility of hybridizing two or more D-FACTS devices can also be considered, and deal with its effect on the improvement of the performance system.
- Further analysis can be performed by considering network reconfiguration, simultaneous placement of DG and D-SATCOM.

References

[1] A. J. Pujara and G. Vaidya, “Voltage stability index of radial distribution network,” *2011 Int. Conf. Emerg. Trends Electr. Comput. Technol. ICETECT 2011*, no. 3, pp. 180–185, 2011.

[2] A. Saranya and S. Dineshkumar, “Improving voltage stability of power system using facts device,” *Proc. - 2017 IEEE Int. Conf. Electr. Instrum. Commun. Eng. ICEICE 2017*, vol. 2017–Decem, pp. 1–5, 2017.

[3] B. G and S. B. CH, “Multi objective Distributed Generators and D-STATCOM sitting and sizing by Modified Particle Swarm Optimization,” *Iarjset*, vol. 2, no. 12, pp. 154–159, 2016.

[4] T. Yuvaraj, K. R. Devabalaji, and K. Ravi, *Optimal Placement and Sizing of DSTATCOM Using Harmony Search Algorithm*, vol. 79. Elsevier B.V., 2015.

[5] T. Yuvaraj, K. Ravi, and K. R. Devabalaji, “DSTATCOM allocation in distribution networks considering load variations using bat algorithm,” *Ain Shams Eng. J.*, vol. 8, no. 3, pp. 391–403, 2017.

[6] R. Sirjani and A. Rezaee Jordehi, “Optimal placement and sizing of distribution static compensator (D-STATCOM) in electric distribution networks: A review,” *Renew. Sustain. Energy Rev.*, vol. 77, no. October 2016, pp. 688–694, 2017.

[7] U. G. Student, S. Medical, S. Medical, T. Sciences, S. Medical, and T. Sciences, “REVIEW ON OPTIMAL ALLOCATION OF DSTATCOM IN RADIAL,” vol. 119, no. 16, pp. 3207–3218, 2018.

[8] M. Farhoodnea, A. Mohamed, H. Shareef, and H. Zayandehroodi, “Power Quality Improvement in Distribution Systems Considering Optimum D-STATCOM Placement,” *J. Kejuruter.*, vol. 25, no. 1, pp. 11–18, 2016.

[9] S. M. S. Hussain and M. Subbaramiah, “An analytical approach for optimal location of DSTATCOM in radial distribution system,” *2013 Int. Conf. Energy Effic. Technol. Sustain. ICEETS 2013*, pp. 1365–1369, 2013.

[10] A. Jain, A. R. Gupta, and A. Kumar, “An efficient method for D-STATCOM placement in radial distribution system,” *India Int. Conf. Power Electron. IICPE*, vol. 2015–May, 2015.

[11] S. A. Taher and S. A. Afsari, “Optimal location and sizing of DSTATCOM in

distribution systems by immune algorithm," *Int. J. Electr. Power Energy Syst.*, vol. 60, pp. 34–44, 2014.

[12] A. I. Technology, K. Kumarasamy, V. Tech, H. Tech, T. Nadu, and T. Nadu, "Cost effective solution for optimal placment and size of multiple statcom using particle swarm optimaztion," vol. 67, no. 3, pp. 701–708, 2014.

[13] M. R. Balu, K. M. Rosalina, and N. P. Kumar, "fuzzy logic based optimal location and sizing of DSTATCOM in radial distribution systems," *Int. J. Adv. Technol. Eng. Sci.*, vol. 2, no. 8, pp. 122–129, 2014.

[14] A. R. Gupta and A. Kumar, "Energy Savings Using D-STATCOM Placement in Radial Distribution System," *Procedia Comput. Sci.*, vol. 70, pp. 558–564, 2015.

[15] K. R. Devabalaji and K. Ravi, "Optimal size and siting of multiple DG and DSTATCOM in radial distribution system using Bacterial Foraging Optimization Algorithm," *Ain Shams Eng. J.*, vol. 7, no. 3, pp. 959–971, 2016.

[16] A. R. Gupta, A. Jain, and A. Kumar, "Optimal D-STATCOM placement in radial distribution system based on power loss index approach," *2015 Int. Conf. Energy, Power Environ. Towar. Sustain. Growth, ICEPE 2015*, pp. 0–4, 2016.

[17] J. Sanam, S. Ganguly, and A. K. Panda, "Allocation of DSTATCOM and DG in distribution systems to reduce power loss using ESM algorithm," *1st IEEE Int. Conf. Power Electron. Intell. Control Energy Syst. ICPEICES 2016*, pp. 1–5, 2017.

[18] M. R. Shaik and A. S. Reddy, "Optimal placement of STATCOM with ABC algorithm to improve voltage stability in power systems," *Int. Conf. Signal Process. Commun. Power Embed. Syst. SCOPES 2016 - Proc.*, pp. 648–652, 2017.

[19] C. S. Hiwarkar and P. G. Burade, "Voltage Stability Enhancement of Power System using STATCOM and SSSC," no. May, pp. 316–320, 2016.

[20] J. P. Navani, N. K. Sharma, and S. Sapra, "Technical and Non-Technical Losses in Power System and Its Economic Consequence in Indian Economy," pp. 757–761, 1956.

[21] A. H. Nizar *et al.*, "With Extreme Learning Machine Method," vol. 23, no. 3, pp. 946–955, 2008.

[22] S. Statistiche, "Detection of non-technical energy losses in power utilities using

data mining techniques."

[23] S. Do Nascimento and M. M. Gouvêa, “Voltage Stability Enhancement in Power Systems with Automatic Facts Device Allocation,” *Energy Procedia*, vol. 107, no. September 2016, pp. 60–67, 2017.

[24] A. Anbarasan and M. Y. Sanavullah, “Voltage Stability Improvement in Power System by Using STATCOM,” *Int. J. Eng. Sci. Technol.*, vol. 4, no. 11, pp. 4584–4591, 2012.

[25] S. Balaji, “Voltage_Stability_Enhancement_by_Optimal,” pp. 1–4, 2014.

[26] C. W. Taylor, “Shunt Compensation for Voltage Stability,” *IFAC Proc. Vol.*, vol. 36, no. 20, pp. 43–48, 2017.

[27] P. Asare, “An Overview of Flexible AC Transmission Systems,” 1994.

[28] A. S. Telang and P. P. Bedekar, “Systematic approach for optimal placement and sizing of STATCOM to assess the voltage stability,” *Proc. IEEE Int. Conf. Circuit, Power Comput. Technol. ICCPCT 2016*, 2016.

[29] E. Ghahremani and I. Kamwa, “Analysing the effects of different types of FACTS devices on the steady-state performance of the Hydro-Québec network,” no. July 2013, pp. 233–249, 2014.

[30] F. Iqbal, M. T. Khan, and A. S. Siddiqui, “Optimal placement of DG and DSTATCOM for loss reduction and voltage profile improvement,” *Alexandria Eng. J.*, vol. 57, no. 2, pp. 755–765, 2018.

[31] A. R. Gupta and A. Kumar, “Optimal placement of D-STATCOM using sensitivity approaches in mesh distribution system with time variant load models under load growth,” *Ain Shams Eng. J.*, vol. 9, no. 4, pp. 783–799, 2018.

[32] P. Balamurugan, “Optimal Allocation of DSTATCOM in Distribution Network Using Whale Optimization Algorithm,” vol. 8, no. 5, pp. 3445–3449, 2018.

[33] R. Sirjani, A. Mohamed, and H. Shareef, “Optimal allocation of shunt Var compensators in power systems using a novel global harmony search algorithm,” *Int. J. Electr. Power Energy Syst.*, vol. 43, no. 1, pp. 562–572, 2012.

[34] C. A. MacDonald and H. J. Dean, “Building connections: The Maestro Project. The evolution of a systems navigator model for transition from pediatric to adult care for young adults with type 1 diabetes,” *Can. J. Diabetes*, vol. 33 (3), p. 315, 2009.

[35] Jen-Hao Teng, “A direct approach for distribution system load flow solutions,” *IEEE Trans. Power Deliv.*, vol. 18, no. 3, pp. 882–887, 2003.

[36] J. Nanda, “Load Flow Algorithms,” vol. 00, no. c, pp. 1157–1161, 2000.

[37] K. Miyazaki and T. Takeshita, “Line loss minimization in radial distribution system using multiple STATCOMs and static capacitors,” *2014 Int. Power Electron. Conf. IPEC-Hiroshima - ECCE Asia 2014*, pp. 601–608, 2014.

[38] B. Singh and M. K. Yadav, “GA for enhancement of system performance by DG incorporated with D-STATCOM in distribution power networks,” *J. Electr. Syst. Inf. Technol.*, no. 2017, 2018.

[39] J. Kennedy and R. Eberhart, “Particle Swarm Optimization,” pp. 1942–1948, 1995.

[40] B. S. Rana and L. Srivastava, “Fuzzy-PSO approach,” *http://ieeexplore.ieee.org/xpl/mostRecentIssue.jsp?punumber=7579440*, 2016.

[41] M. H. Moradi and M. Abedini, “A combination of genetic algorithm and particle swarm optimization for optimal distributed generation location and sizing in distribution systems with fuzzy optimal theory,” *Int. J. Green Energy*, vol. 9, no. 7, pp. 641–660, 2012.

[42] G. Gowtham and a. L. Devi, “Power Loss Reduction and Voltage Profile Improvement by DSTATCOM using PSO,” *Int. J. Eng. Res. Technol.*, vol. Vol. 4, no. Issue 02, pp. 192–196, 2015.

[43] W. F. Abd-El-Wahed, A. A. Mousa, and M. A. El-Shorbagy, “Integrating particle swarm optimization with genetic algorithms for solving nonlinear optimization problems,” *J. Comput. Appl. Math.*, vol. 235, no. 5, pp. 1446–1453, 2011.

[44] Y. Del Valle, J. C. Hernandez, G. K. Venayagamoorthy, and R. G. Harley, “Multiple STATCOM allocation and sizing using Particle Swarm Optimization,” *2006 IEEE PES Power Syst. Conf. Expo. PSCE 2006 - Proc.*, pp. 1884–1891, 2006.

[45] G. Niazi and M. Lalwani, “PSO based optimal distributed generation placement and sizing in power distribution networks: A comprehensive review,” *2017 Int. Conf. Comput. Commun. Electron. COMPTELIX 2017*, no. 1, pp. 305–311, 2017.

[46] P. Delivery and S. Member, “Calculation of Overhead Transmission Line Impedances A Finite Element Approach,” vol. 14, no. 1, 1999.

[47] P. Grid, “Calculating Sequence Impedances of Transmission Line Using PMU Measurements,” 2015.

[48] J. Modarresi, E. Gholipour, and A. Khodabakhshian, “A comprehensive review of the voltage stability indices,” *Renew. Sustain. Energy Rev.*, vol. 63, pp. 1–12, 2016.

[49] R. B. Prada *et al.*, “Identification of weak buses using Voltage Stability Indicator and its voltage profile improvement by using DSTATCOM in radial distribution systems,” *IEEE Trans. Power Syst.*, vol. 2, no. 4, pp. 392–396, 2013.

[50] M. Okati and M. Aminian, “Distribution System Loss Reduction , Voltage Profile and Stability Improvement by Determining the Optimal Size and Location of D-Statcom,” vol. 4, no. 2, pp. 67–80, 2017.

[51] J. K. Charles and N. A. Odero, “A combined sensitivity factor based GA-IPSO approach for system loss reduction and voltage profile enhancement,” vol. 12, no. 2, 2013.

[52] M. Akhtar and L. Mathew, “Cost Comparison of FACTS Devices for Industrial Application – A study,” vol. 1, no. 4, pp. 39–46, 2016.

[53] http://ethioenergybuz.com/power-sector/electricity-transaction/165-electricity-tariff-ethiopia, 2019

[54] http://sinopakelectric.diytrade.com/

APPENDIX

APPENDIX A: Base case load flow algorithm program

```
function[finalres]=load_flow_after_dsat(nbus,Dsat_place,data_pass_to_l
oadflow)
voltage_minimum=data_pass_to_loadflow{1};
voltage_maximum=data_pass_to_loadflow{2};
capmaxsij_maximum=data_pass_to_loadflow{3};
source_num=[1];
[LINEDATA]=linedata_radial_bus(nbus);
BUSDATA=busdata_radial_bus(nbus);
baseKV=15;baseMVA=100;
PBASE=baseMVA*1000;VBASE=(baseKV^2)/baseMVA;
busdata_value=BUSDATA;linedata_value=LINEDATA;
linedata_value(:,4:5)=linedata_value(:,4:5)/VBASE;
resistance_val=linedata_value(:,4);
reactance_val=linedata_value(:,5);
actual_imped=complex(resistance_val,reactance_val);
busdata_value(:,2:3)=1.5*(busdata_value(:,2:3)/PBASE);
imped_value=actual_imped;
[bibc_matrix]=bibc_gen(linedata_value,busdata_value);
bibc_matrix(source_num,:)=[];
bibc_matrix(:,source_num)=[];
final_bibc_matrix=bibc_matrix';
final_bcbv_matrix=final_bibc_matrix'*diag(actual_imped);
final_dlf_matrix=final_bcbv_matrix*final_bibc_matrix;
complex_load_d=complex(busdata_value(:,2),busdata_value(:,3));%
complex power load
complex_load_g=zeros(size(busdata_value,1),1);
Dsat_place;
loc_value=round(Dsat_place(1));
dsat_value=Dsat_place(2);
for ind=1:length(loc_value)
        PG=0;
        QG=(dsat_value(ind));
        complex_load_g(loc_value(ind))=complex(PG/PBASE,QG/PBASE);
end
final_load_matrix=(complex_load_d-complex_load_g);
final_load_matrix(length(source_num))=[];
initial_volt_value=ones(size(busdata_value,1)-length(source_num),1);%
initial bus voltage
voltage_drop_value=initial_volt_value;
max_iter=300;
for ind_lop=1:max_iter
    %backward sweep
    inject_current_data=conj(final_load_matrix./voltage_drop_value); %
injected current at each bus
    IB=final_bibc_matrix*inject_current_data; %get the cumulative
injected current flowing through each branch
    old_volt=voltage_drop_value;
    volt_drop_each=final_dlf_matrix*inject_current_data; %voltage
drops along each branch.
    voltage_drop_value=initial_volt_value-volt_drop_each;
    old_volt1=(old_volt);
    new_volt=(voltage_drop_value);
    error_volt_tolr=max(abs(old_volt1-new_volt));
end
```

```
final_volt_data=[ones(length(source_num),1);voltage_drop_value];
rvolt=real(final_volt_data);ivolt=imag(final_volt_data);
scv=sum(double(length(find((rvolt<voltage_minimum) |
(rvolt>voltage_maximum)))).^2);
locvoltm=find(rvolt>voltage_maximum);rvolt(locvoltm)=voltage_maximum;
locvoltm=find(rvolt<voltage_minimum);rvolt(locvoltm)=voltage_minimum;
final_volt_data=complex(rvolt,ivolt);
from_node=linedata_value(:,2);
to_node=linedata_value(:,3);
for ind=1:length(from_node)
    volt_diff_value(ind,:)=final_volt_data(from_node(ind))-
final_volt_data(to_node(ind));
end
volt_diff_value1=abs(volt_diff_value);
ploss=((volt_diff_value1.^2).*resistance_val)./(abs(imped_value).*abs(
imped_value))*10^5; % Each Line Loss in kWs
loc1=find(~(isnan(ploss)));
locp=find(ploss>capmaxsij_maximum);
ploss(locp)=capmaxsij_maximum;
qloss=((volt_diff_value1.^2).*reactance_val)./(abs(imped_value).*abs(i
mped_value))*10^5; % Each Line Loss in kVAr
loc2=find(~(isnan(qloss)));
power_loss=sum(ploss(loc1));
total_reactive_loss=sum(qloss(loc2));
finalvoltage=real(final_volt_data);
cost_loss=0.06; %dollar/kwh;
Hours_in_year=8760;% hrs
Anual_loss=power_loss*cost_loss*Hours_in_year;
f1=power_loss;
f2=sum((1-finalvoltage).^2);
    %% vsi calculation
    for kk=1:length(busdata_value(:,2))
        for ki=1:length(linedata_value(:,4))

vsival(kk)=(abs(finalvoltage(kk)).^4)(4*(busdata_value(kk,2)*linedata_
value(ki,4)-busdata_value(kk,3)*linedata_value(ki,5)).^2)
((4*(busdata_value(kk,2)*linedata_value(ki,5)busdata_value(kk,3)*lined
ata_value(ki,4)).^2)*finalvoltage(kk).^2);
        end
    end
f3=min(vsival);
w1=0.8;
w2=0.1;
w3=0.1;
final_obj=w1*f1+w2*f2+w3*(1/f3);
finalres{1}=final_obj;
finalres{2}=power_loss;
finalres{3}=finalvoltage;
finalres{4}=vsival;
finalres{5}=min(vsival);
finalres{6}=total_reactive_loss;
finalres{7}=finalvoltage;
finalres{8}=min(finalvoltage);
finalres{9}=max(finalvoltage);
finalres{10}=max(vsival);
finalres{11}=ploss;
finalres{12}=qloss;
finalres{13}=Anual_loss
```

APPENDIX B: Particle swarm optimization program

```
clc
clear all
close all
%% PSO algorithm
nbus=59;
voltage_minimum=0.95;
voltage_maximum=1.05;
capmaxsij_maximum=100;
QMIN_VALUE=100;
QMAX_VALUE=1250;
data_pass_to_loadflow{1}=voltage_minimum;
data_pass_to_loadflow{2}=voltage_maximum;
data_pass_to_loadflow{3}=capmaxsij_maximum;
dsatcom_num=1; % no of Dstatcom
[finalres_base_case]=load_flow_base(nbus);% load flow for base case
no_of_variables=(dsatcom_num*2);
min_max_value_range=ones(no_of_variables,2); %set limits for random
particle value
dsat_qmin=QMIN_VALUE; % minimum size
dsat_qmax=QMAX_VALUE; % maximum size
for kr=1:1
    min_max_value_range(kr,1)=1; %set lower value
    min_max_value_range(kr,2)=nbus; %set upper value
end
for kr=2:no_of_variables
    min_max_value_range(kr,1)=dsat_qmin; %set lower value
    min_max_value_range(kr,2)=dsat_qmax; %set upper value
end
maxiter=30;  % set number of iteration
initial_population_size=30; % set population size
initial_pso_seed=zeros(initial_population_size,no_of_variables); %
create zero matrix
% randmoly generate initial value
for kr=1:initial_population_size
    for kc=1:1
        initial_pso_seed(kr,kc)=randsrc(1,1,1:nbus);
    end
    for kc=2:no_of_variables
        initial_pso_seed(kr,kc)=dsat_qmin+((dsat_qmax-
dsat_qmin)*rand(1,1));
    end

end
% call pso function
[psooutput]=PSO_PROCESS_FUNC(nbus,no_of_variables,...
    2 ,min_max_value_range,...
    initial_population_size,maxiter,data_pass_to_loadflow);
 finalresult_val=psooutput(1:no_of_variables);
D_loc=round(finalresult_val(1));
D_SIZE=finalresult_val(2);
Dsat_place=[D_loc;D_SIZE];
[finalres_after_comp]=load_flow_after_dsat(nbus,Dsat_place,data_pass_t
o_loadflow);
%% display final result
display('PSO RESULTS ');
POWER_LOSS_BASE_CASE=finalres_base_case{2}
VSI_MINIMUM_BASE_CASE=finalres_base_case{5}
Reactive_power_loss_base_case=finalres_base_case{6}
```

```
D_STATCOM_LOCATION=D_loc
D_STATCOM_SIZE_kVAr=D_SIZE
POWER_LOSS_WITH_DSTATCOM=finalres_after_comp{2}
Reactive_power_loss_with_DSTACOM=finalres_after_comp{6}
VSI_MINIMUM_WITH_DSTATCOM=finalres_after_comp{5}
Active_power_loss_percantage_reduction=(POWER_LOSS_BASE_CASE-
POWER_LOSS_WITH_DSTATCOM)/(POWER_LOSS_BASE_CASE)*100%
Reactive_power_loss_percenatge_reduction=(Reactive_power_loss_base_cas
e-
Reactive_power_loss_with_DSTACOM)/(Reactive_power_loss_base_case)*100%
Minimum_voltage_base_case=finalres_base_case{8}
Minimum_voltage_after_dstatcom=finalres_after_comp{8}
Annual_loss_expense_base_case=finalres_base_case{13}
Annual_loss_expense_after_dstatcom=finalres_after_comp{13}
voltage_profile_base_case=finalres_base_case{7}
voltage_profile_after_dstatcom=finalres_after_comp{7}
voltage_stablity_index_base_case=finalres_base_case{4}
voltage_stablity_index_after_dstatcom=finalres_after_comp{4}
Active_power_loss_buses_WITH_OUT_DSTATCOM=finalres_base_case{11}
Active_power_loss_buses_WITH_DSTATCOM=finalres_after_comp{11}
Reactive_power_loss_buses_WITH_OUT_DSTATCOM=finalres_base_case{12}
Reactive_power_loss_buses_WITH_DSTATCOM=finalres_after_comp{12}
voltage_before_compensation=finalres_base_case{3};
voltage_stab_index_before_compensation=finalres_base_case{4};
voltage_after_compensation=finalres_after_comp{3};
voltage_stab_index_after_compensation=finalres_after_comp{4};
figure,plot(1:nbus,voltage_before_compensation,'r-s');
hold on,plot(1:nbus,voltage_after_compensation,'k-o');
xlabel('Bus Number');
ylabel('Voltage');
grid on;
legend('BASE CASE','WITH D-STATCOM');
title('Voltage Profile of the System Before and After Compensation');
figure,plot(1:nbus,voltage_stab_index_before_compensation,'r-s');
hold on,plot(1:nbus,voltage_stab_index_after_compensation,'k-o');
xlabel('Bus Number');
ylabel('Voltage Stability Index');
grid on;
legend('BASE CASE','WITH D-STATCOM');
title('Voltage Stability Index for All Buses');
xlswrite('voltage_stability_index_value_before_compensation_PSO.xls',.
..voltage_stab_index_before_compensation.');
xlswrite('voltage_stability_index_value_after_compensation_PSO.xls',..
.voltage_stab_index_after_compensation.');
 xlswrite('voltage_profile_before_compensation_PSO.xls',...
    voltage_before_compensation);
 xlswrite('voltage_profile_after_compensation_PSO.xls',...
    voltage_after_compensation);
```

APPENDIX C: Load and line data of Papyrus feeder

Sending node	Receiving node	Conductor type	Length (km)	Resistance (Ω)	Reactance (Ω)	Pload receiving (kw)	Load receiving (KVAr)
1	2	AAC95	1.516	0.46	0.49	198	129.5
1	3	AAC95	0.791	0.24	0.25	175.2	124
3	4	AAC95	1.379	0.42	0.44	125	99
3	5	AAC95	0.458	0.14	0.13	105	79
5	6	AAC25	0.465	0.54	0.17	90.5	68
5	7	AAC25	0.563	0.66	0.21	118.69	88
5	8	AAC95	0.518	0.15	0.16	130.56	94
8	9	AAC95	0.33	0.10	0.11	0	0
9	10	AAC95	0.517	0.15	0.16	50	38
9	11	AAC95	0.379	0.11	0.12	80	57
8	12	AAC95	0.339	0.13	0.10	87	52
12	13	AAC95	0.246	0.07	0.08	0	0
13	14	AAC50	1.828	1.05	0.63	100	75
13	15	AAC50	0.645	0.37	0.22	86	50
12	16	AAC50	0.699	0.40	0.24	81	45
16	17	AAC95	1.879	0.57	0.60	90	54
16	18	AAC95	0.699	0.21	0.22	78.6	46
18	19	AAC95	0.761	0.23	0.24	49	28
18	20	AAC95	0.769	0.23	0.24	70	45
20	21	AAC25	0.592	0.69	0.22	90	58
20	22	AAC50	0.314	0.18	0.10	30	21.08
22	23	AAC50	0.48	0.27	0.16	15	6.5
22	24	AAC25	0.397	0.46	0.14	70.8	50
24	25	AAC50	0.498	0.28	0.17	0	0
24	26	AAC95	0.753	0.23	0.24	0	0
26	27	AAC50	0.482	0.27	0.16	70	50.5
26	28	AAC95	1.059	0.32	0.34	80	55.05
28	29	AAC50	2.591	1.49	0.89	85.5	53.5
28	30	AAC95	0.271	0.08	0.09	0	0
30	31	AAC25	2.047	2.41	0.76	68	38
31	32	AAC95	0.891	0.27	0.28	75	35.5
32	33	AAC50	1.398	0.80	0.40	80	48.5
32	34	AAC25	1.469	1.73	0.54	70	26.3
34	35	AAC25	0.54	0.63	0.20	40.5	16.5
34	36	AAC25	1.269	1.49	0.20	60	35.5
30	37	AAC95	0.453	0.13	0.14	90	45.8
37	38	AAC25	0.43	0.50	0.16	70	38.09
38	39	AAC25	0.512	0.60	0.19	75	39
38	40	AAC25	0.427	0.50	0.15	83	55.6
40	41	AAC25	0.649	0.76	0.24	68	44.5
40	42	AAC50	0.389	0.22	0.13	67	48.5
37	43	AAC95	0.67	0.20	0.21	0	0
43	44	AAC25	1.45	1.71	0.54	58	39.40
44	45	AAC50	0.413	0.23	0.14	82	49
44	46	AAC25	0.914	1.07	0.34	90.35	58.5

43	47	AAC50	0.401	0.23	0.13	85	47.04
47	48	AAC50	0.442	0.25	0.15	0	0
47	49	AAC50	0.447	0.25	0.15	83	45.8
49	50	AAC50	0.391	0.22	0.13	0	0
49	51	AAC50	0.462	0.26	0.16	74	38.3
51	52	AAC50	0.307	0.17	0.10	96	55.2
51	53	AAC95	0.443	0.13	0.14	0	0
53	54	AAC95	0.345	0.10	0.11	84.08	49
53	55	AAC95	0.126	0.03	0.04	0	0
55	56	AAC95	1.054	0.32	0.34	90	59
55	57	AAC50	0.391	0.22	0.13	0	0
57	58	AAC50	0.42	0.24	0.14	96	58
57	59	AAC50	0.403	0.23	0.13	109	88

APPENDIX D: single line diagram of papyrus feeder

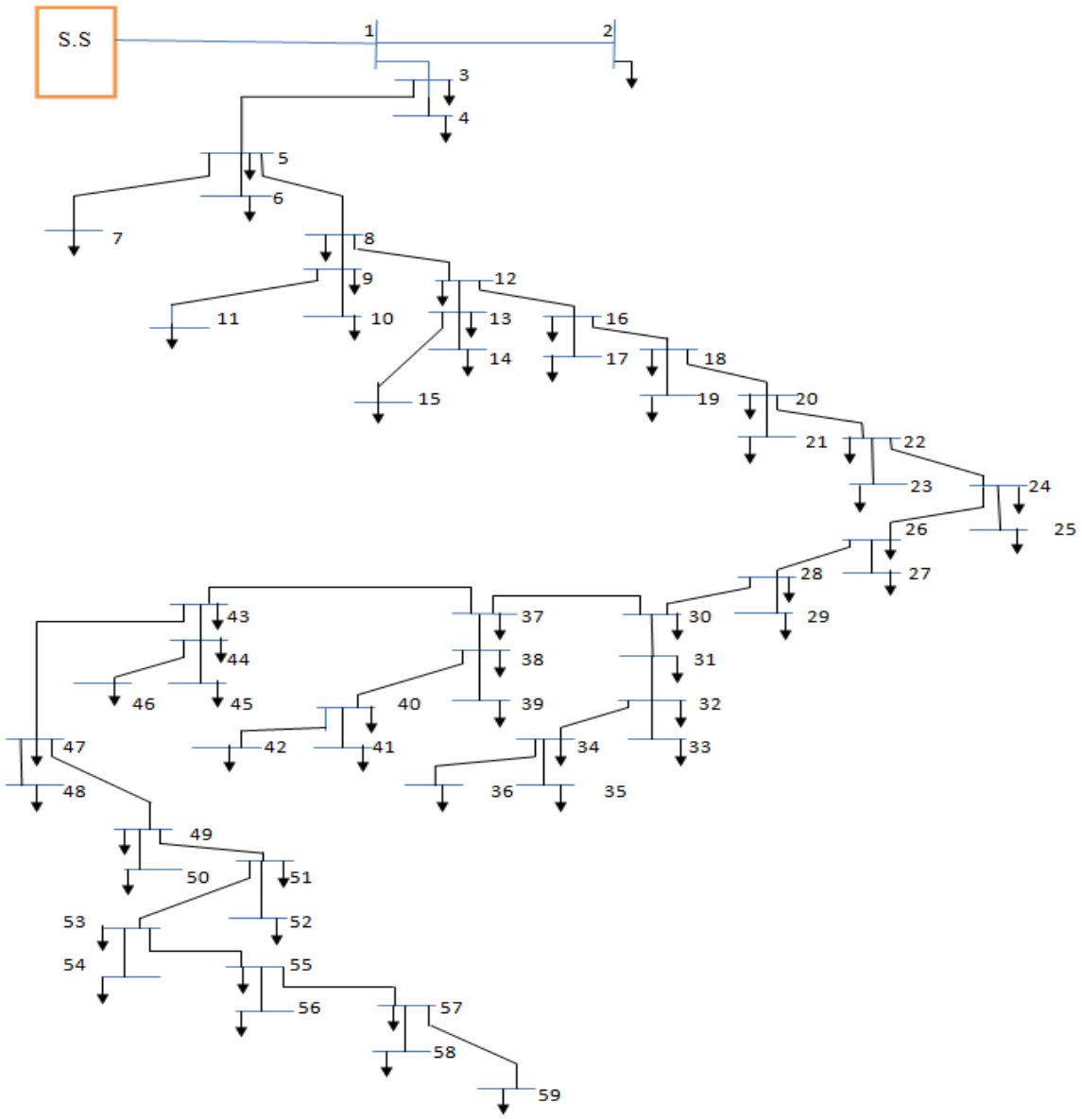

APPENDIX E: Tarrif 10

Domestic: /tariff 10/;

This tariff category consists of the service the utility provides to residential consumption. The consumer energy demand for this kind of service is limited to few KWs. One peculiar provision in the domestic tariff category which is not available with the rest of the categories other than the commercial category/which has two different tariff ranges/ is that it includes ranges of tariff categories. The intention of this range of categories which has an increasing value as the KWH consumption rises is to protect the low level energy consumers.

Table 1.1: E nergy/KWH:-

No	category	Monthly Consumption range	Rate/Eth Birr
1	1st block	0-50	0.273
2	2nd block	51-100	0.3564
3	2nd block	101-200	0.4993
4	4th block	201-300	0.5500
5	5th block	301-400	0.5666
6	6th block	401-500	0.5880
7	7th block	>500	0.6943

Table 1.2: Service charge:

No	Type of service	Monthly Consumption range	Rate/Eth Birr

APPENDIX F: 15kV 1.25Mvar STATCOM Technical Specifications

Rated voltage	15kV±10%
Rated current	48A
Input voltage range	15KV 0.15～1.2Pu
Grid frequency	50±0.5Hz
Power loss at full load	<2kW
THDi	≤3% based on GB/T14549-1993
PCC THDu	≤3% based on GB/T14549-1993
Response time	<5ms
Overload ability	1.1times continues operation give alarm after 3 minutes 1.2times trip after 1 minute 1.3times trip instantaneously
Steady-state accuracy	2.5%
Fault resolve	Power Module Redundancy design, Enables built in n+1 configurations by adding a spare module to achieve breakthrough levels in power availability
Operation mode	Constant reactive power, Constant voltage, Constant pf, Harmonic current cancellation, load compensation
Communication interface	RS485, Ethernet/Modbus, IEC104
Monitor mode	Local/Remote
HMI	LCD
Signal transmission	Optic-fiber
Modulation mode	Single Polarity Double Frequency, carrier phase-shifted S-PWM

15KV Container Typed SVG Photos for reference

Outdoor Installation

Power Modules in Container

Control panel in Container

Isolation switch Soft-starting isolation switch Connection reactor

Outdoor installation